

# Spatial transcriptomic for studying neurodegenerative diseases

Giulia Miracca

Journal Club

30/03/2021



# The positional context of transcripts is key

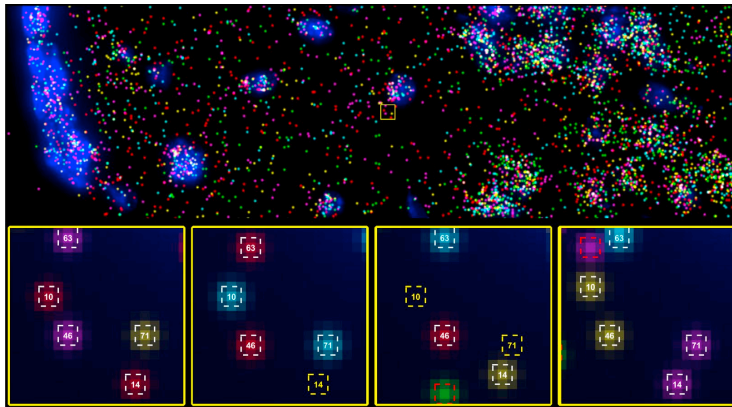
- Previously RNA-seq data were performed on biopsies and tissue homogenates giving average transcriptome information
- The localization of transcript expression is essential for interrogating tissue functionality and pathological changes
- Combination of presence or absence of expression of a set of genes with their localization can be used to define marker profiles both anatomically and in pathological conditions



# Just before spatial transcriptomic

Previous attempts have focused on scaling up Fluorescent In-Situ Hybridization (FISH):

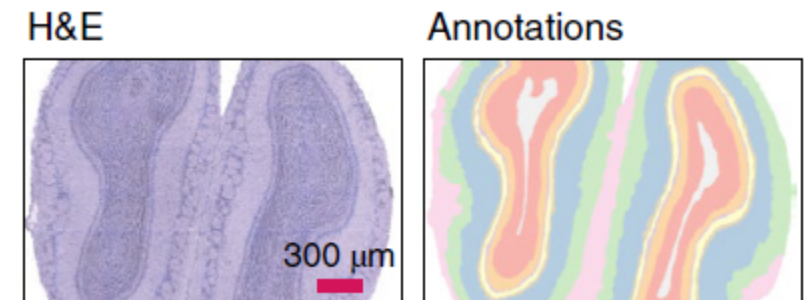
- MERFISH: single molecule imaging approach using combinatorial FISH labeling and sequential imaging
- seqFISH: sequential probe hybridizations for pre-defined temporal sequence of colors, generating in situ mRNA barcodes



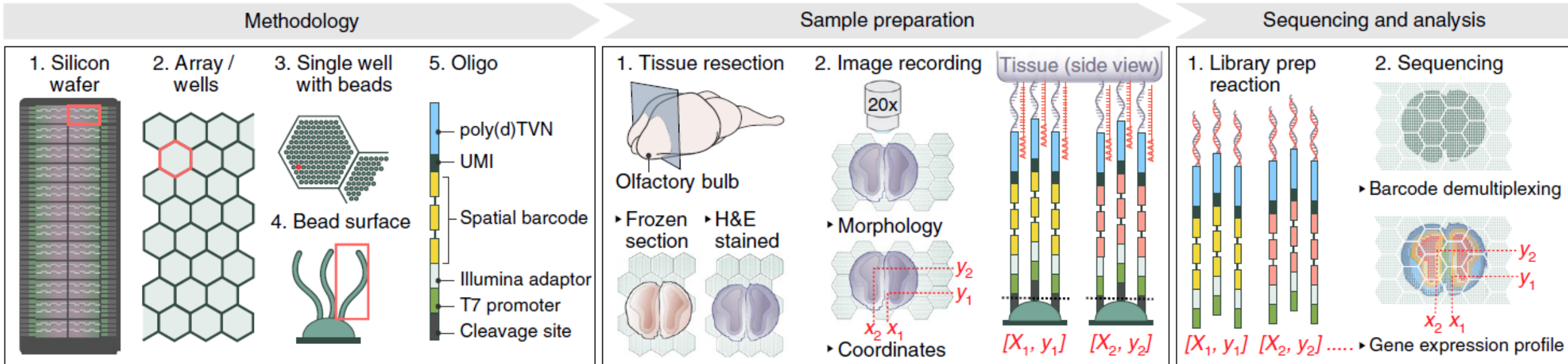
# Spatial transcriptomic

**Allows the visualization and quantitative analysis of the transcripts with spatial resolution in individual tissue sections**

- ST gives quantitative transcriptome-wide RNA-seq data thanks to spatially barcoded capture DNA probes distributed on slide arrays
- After “on slide” reverse transcription, cDNA is released from the slide and sequenced
- Thanks to the barcodes one can reconstruct the localization of the transcripts based on their localization on the slide/array
- RNA distribution can be mapped on images of the tissues taken before reverse transcription
- This is compatible with multiple Ab IHC and H&E staining



# Example of ST workflow



Vickovic et al., *Nat Methods* (2019)

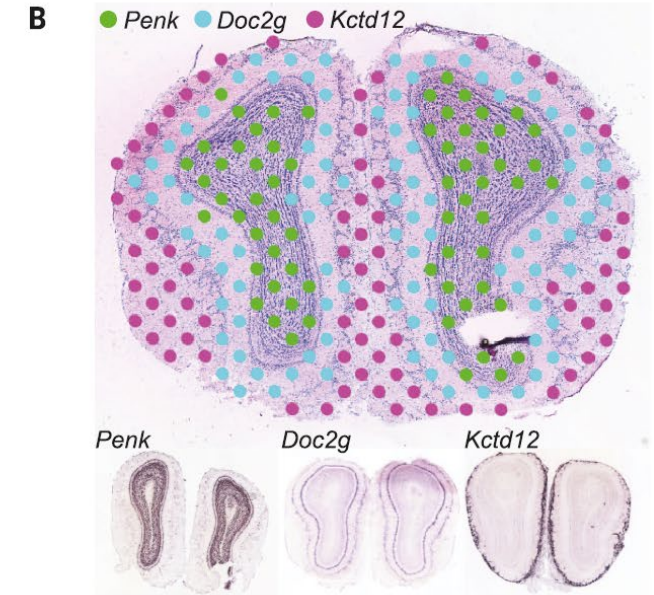
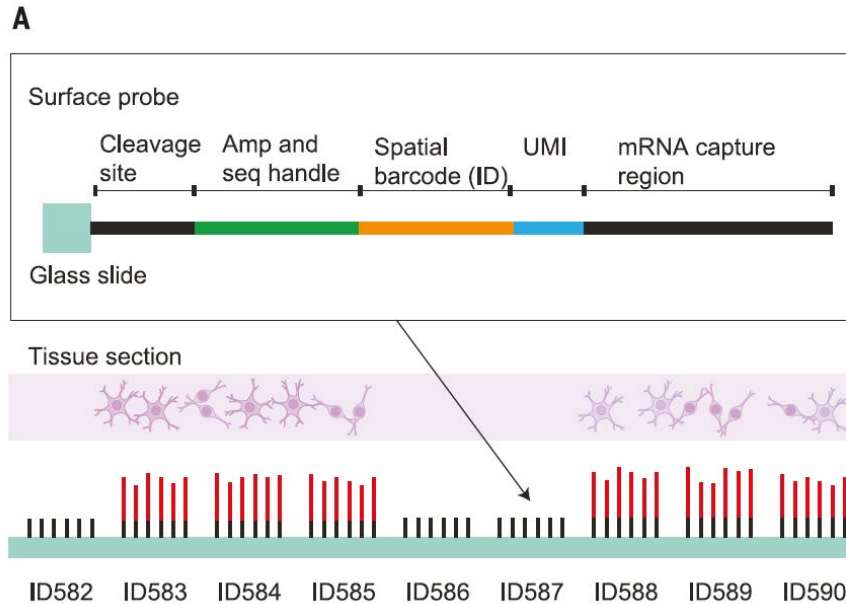
- Capture oligos are placed on a slide array
- Tissue is sliced, stained and imaged
- After hybridization and reverse transcription, the oligos carrying the cDNA are cleaved and sequenced
- The oligos are mapped back into their spatial distribution to be then overlapped with imaging data

# First publications of ST on brain tissue

## Visualization and analysis of gene expression in tissue sections by spatial transcriptomics

Patrik L. Ståhl,<sup>1,2\*</sup> Fredrik Salmén,<sup>2\*</sup> Sanja Vickovic,<sup>2†</sup> Anna Lundmark,<sup>2,3†</sup> José Fernández Navarro,<sup>1,2</sup> Jens Magnusson,<sup>1</sup> Stefania Giacomello,<sup>2</sup> Michaela Asp,<sup>2</sup> Jakub O. Westholm,<sup>4</sup> Mikael Huss,<sup>4</sup> Annelie Mollbrink,<sup>2</sup> Sten Linnarsson,<sup>5</sup> Simone Codeluppi,<sup>5,6</sup> Åke Borg,<sup>7</sup> Fredrik Pontén,<sup>8</sup> Paul Igor Costea,<sup>2</sup> Pelin Sahlén,<sup>2</sup> Jan Mulder,<sup>9</sup> Olaf Bergmann,<sup>1</sup> Joakim Lundeberg,<sup>2†</sup> Jonas Frisén<sup>1</sup>

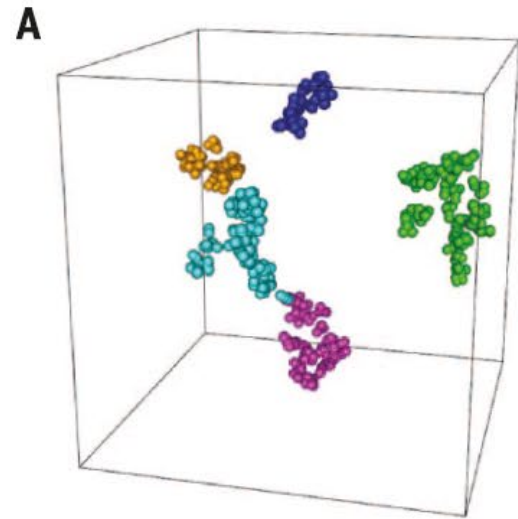
SCIENCE 1 JULY 2016 • VOL 353 ISSUE 6294



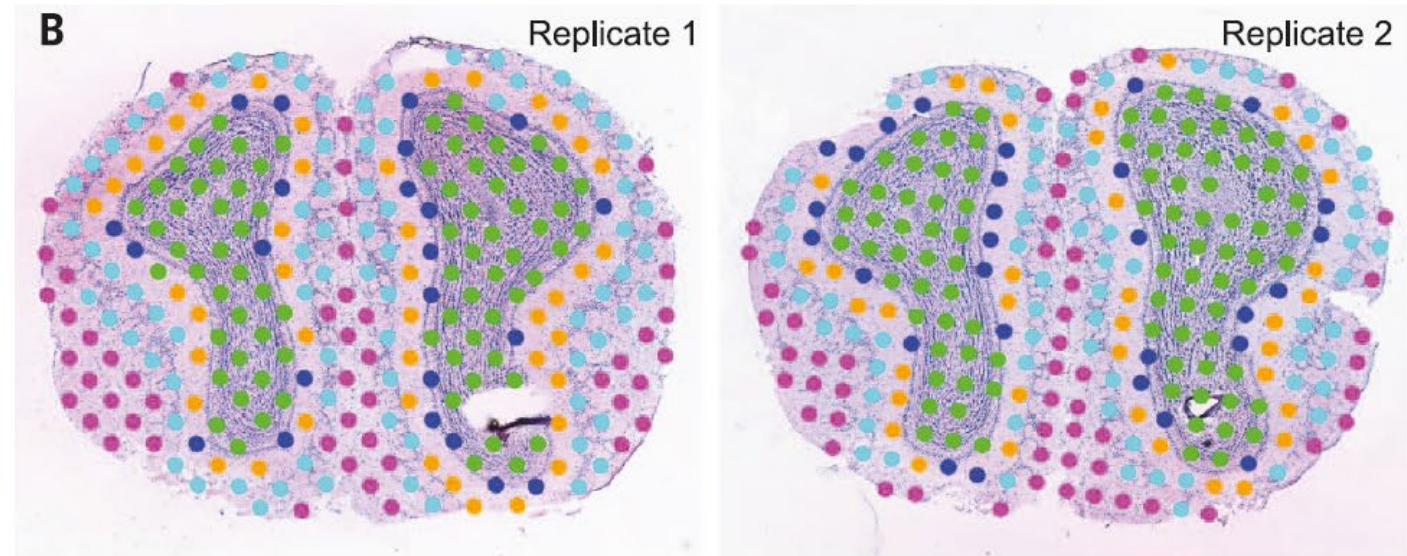
→ 100  $\mu\text{m}$  capturing areas, distanced from each other of other 100  $\mu\text{m}$

→ ST gene expression corresponded to *in situ* hybridization data, confirming its sensitivity

# Comparative analysis of tissue domains



● Cluster 1: Granular cell layer  
● Cluster 2: Mitral cell layer



● Cluster 3: Outer plexiform layer  
● Cluster 4: Glomerular layer

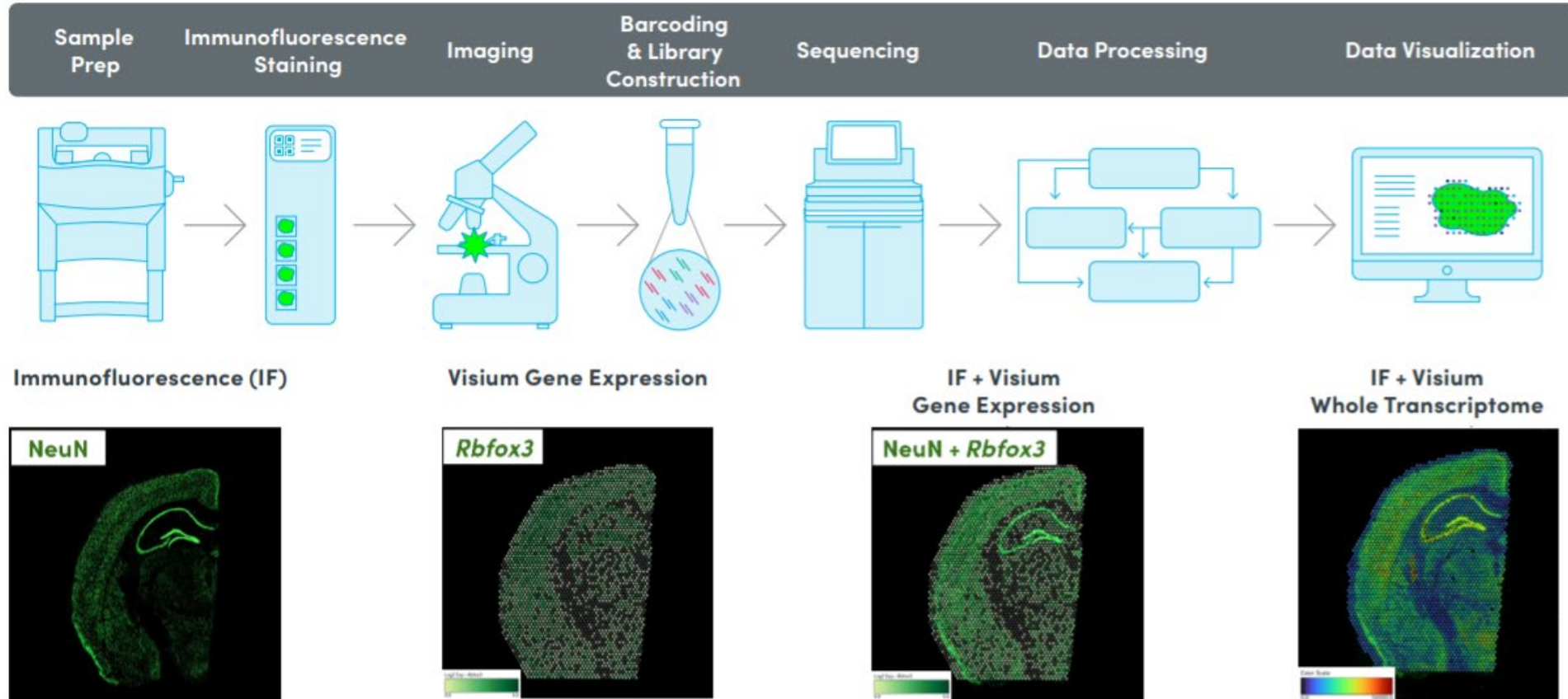
● Cluster 5: Olfactory nerve layer

Exploration of gene expression profiles in spatially defined domains in the olfactory bulbs:

→ t-SNE dimensionality reduction, followed by hierarchical clustering

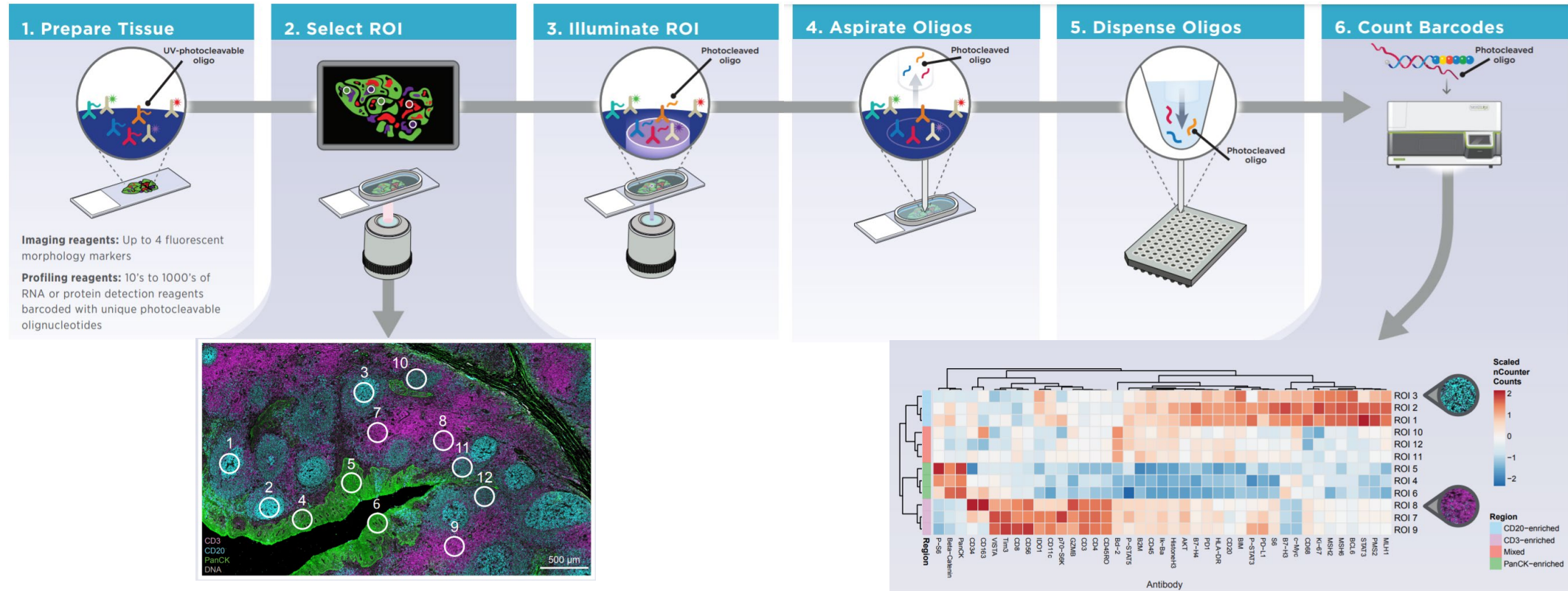
→ The clustered features corresponded to the OB morphological layers when placed back on tissue images

# Commercialization of ST: 10x genomics



- One-day lab workflow
- 1-10 cell resolution per spot (55  $\mu\text{m}$ )
- Offers targeted gene expression panels if not interested in whole transcriptome analysis
- Available with protein co-detection

# Commercialization of ST: nanoString



- Developed on paraffin embedded tissues
- Limited amounts of probes but for both RNA and protein detection → promoting now whole transcriptome
- Does not analyze whole tissue sections but only ROIs
- Needs specialized equipment

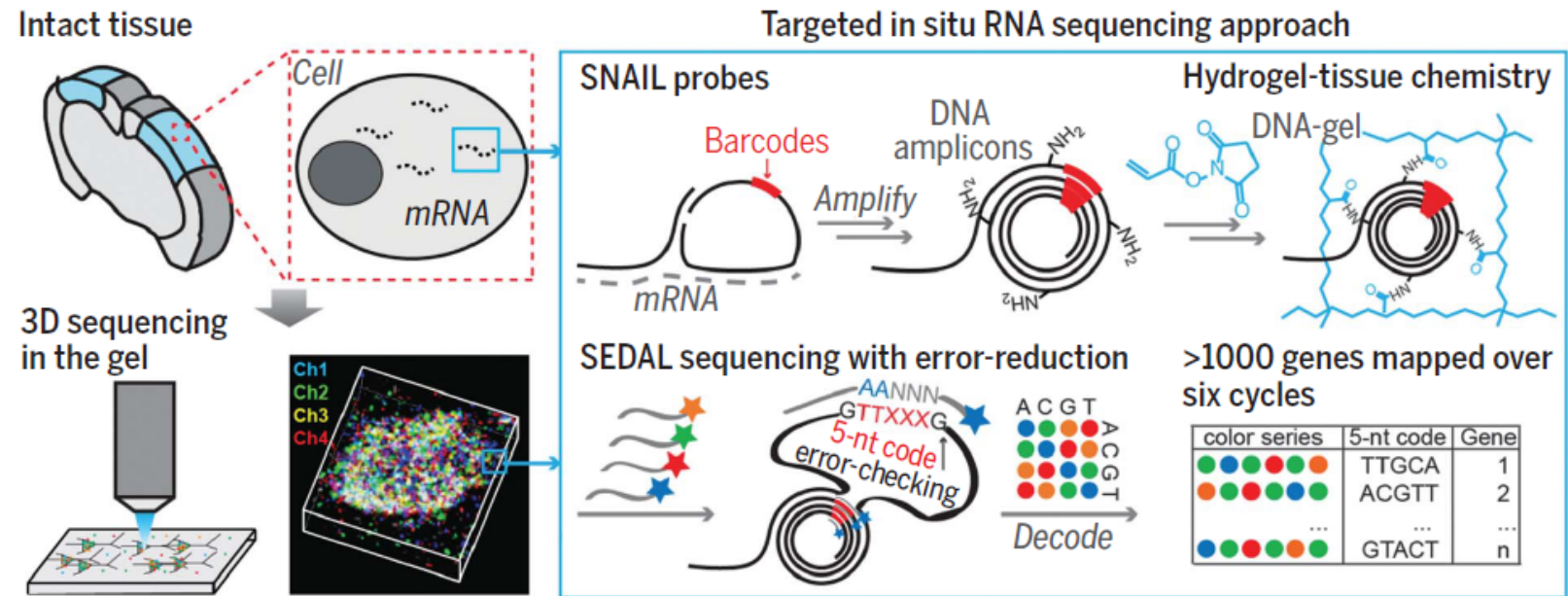
# Numerous labs have also developed their own ST protocol: STARmap

## Three-dimensional intact-tissue sequencing of single-cell transcriptional states

Xiao Wang\*, William E. Allen\*, Matthew A. Wright, Emily L. Sylwestrak, Nikolay Samusik, Sam Vesuna, Kathryn Evans, Cindy Liu, Charu Ramakrishnan, Jia Liu, Garry P. Nolan†, Felice-Alessio Bava†, Karl Deisseroth†

*Science* 361, 380 (2018)

- Gives results in 3D thanks to the *in-situ* sequencing in hydrogel
- Not yet transcriptome-wide → barcodes are specific for the gene and not for the location
- You destroy the tissue after the protocol (not reusable)



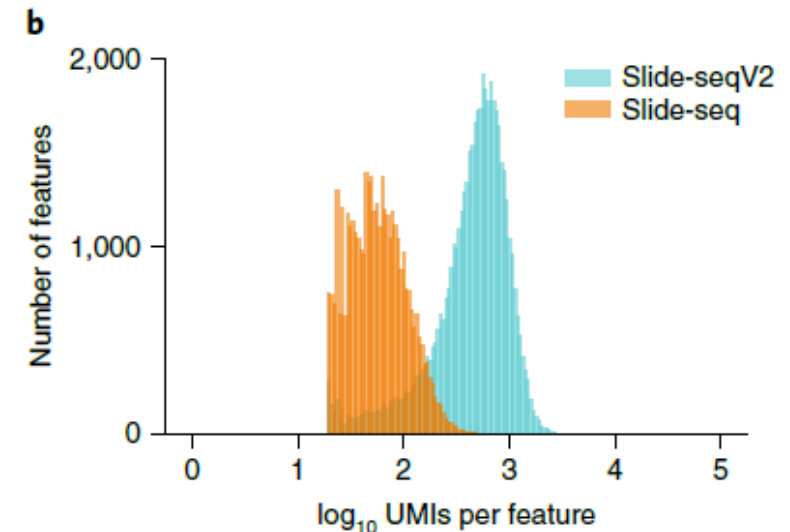
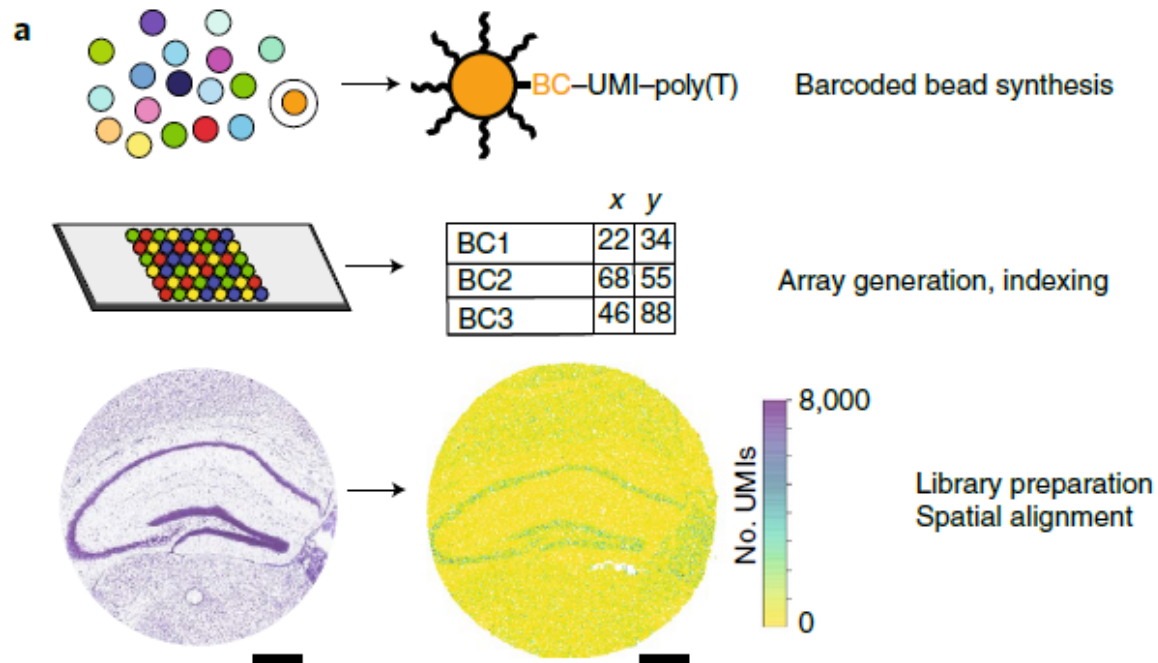
# Slide-SeqV2

## Highly sensitive spatial transcriptomics at near-cellular resolution with Slide-seqV2

Robert R. Stickels<sup>1,2,3,6</sup>, Evan Murray<sup>1,6</sup>, Pawan Kumar<sup>1</sup>, Jilong Li<sup>1</sup>, Jamie L. Marshall<sup>1</sup>, Daniela J. Di Bella<sup>4</sup>, Paola Arlotta<sup>5</sup>, Evan Z. Macosko<sup>1,5,7</sup> and Fei Chen<sup>1,4,7</sup>

NATURE BIOTECHNOLOGY | VOL 39 | MARCH 2021 | 313-319

- Unbiased transcriptome-scale profiling on large areas
- Use on densely barcoded bead arrays indexed before placing the tissue on them
- Near to cellular resolution (10 $\mu$ m vs 55 with 10x genomics)



# How to apply ST on neurodegenerative diseases?

Two examples based on 10x genomics technique, predominantly on mouse tissue and related to neurodegenerative diseases

## Paper #1

### Spatiotemporal dynamics of molecular pathology in amyotrophic lateral sclerosis

Silas Maniatis<sup>1\*</sup>, Tarmo Äijö<sup>2\*</sup>, Sanja Vickovic<sup>1,3,4\*</sup>, Catherine Braine<sup>1,5</sup>, Kristy Kang<sup>1</sup>, Annelie Mollbrink<sup>4</sup>, Delphine Fagegaltier<sup>1</sup>, Žaneta Andrusivová<sup>4</sup>, Sami Saarenpää<sup>4</sup>, Gonzalo Saiz-Castro<sup>4</sup>, Miguel Cuevas<sup>5</sup>, Aaron Watters<sup>2</sup>, Joakim Lundeberg<sup>4,6†</sup>, Richard Bonneau<sup>2,7†</sup>, Hemali Phatnani<sup>1,5†</sup>

*Science* **364**, 89–93 (2019)

## Paper #2

### Spatial Transcriptomics and *In Situ* Sequencing to Study Alzheimer's Disease

Wei-Ting Chen,<sup>1,2,11</sup> Ashley Lu,<sup>1,2,11</sup> Katleen Craessaerts,<sup>1,2</sup> Benjamin Pavie,<sup>1,2,3,4</sup> Carlo Sala Frigerio,<sup>1,2,10</sup> Nikky Corthout,<sup>1,2,3,4</sup> Xiaoyan Qian,<sup>5</sup> Jana Laláková,<sup>5</sup> Malte Kühnemund,<sup>5</sup> Iryna Voytyuk,<sup>1,2</sup> Leen Wolfs,<sup>1,2</sup> Renzo Mancuso,<sup>1,2</sup> Evgenia Salta,<sup>1,2</sup> Sriram Balusu,<sup>1,2</sup> An Snellinx,<sup>1,2</sup> Sebastian Munck,<sup>1,2,3,4</sup> Aleksandra Jurek,<sup>6</sup> Jose Fernandez Navarro,<sup>6</sup> Takaomi C. Saido,<sup>7</sup> Inge Huitinga,<sup>8,9</sup> Joakim Lundeberg,<sup>6</sup> Mark Fiers,<sup>1,2,10,\*</sup> and Bart De Strooper<sup>1,2,10,12,\*</sup>

Cell 182, 976–991, August 20, 2020

# Spatiotemporal dynamics of molecular pathology in amyotrophic lateral sclerosis

Maniatis et al., *Science* **364**, 89–93 (2019)

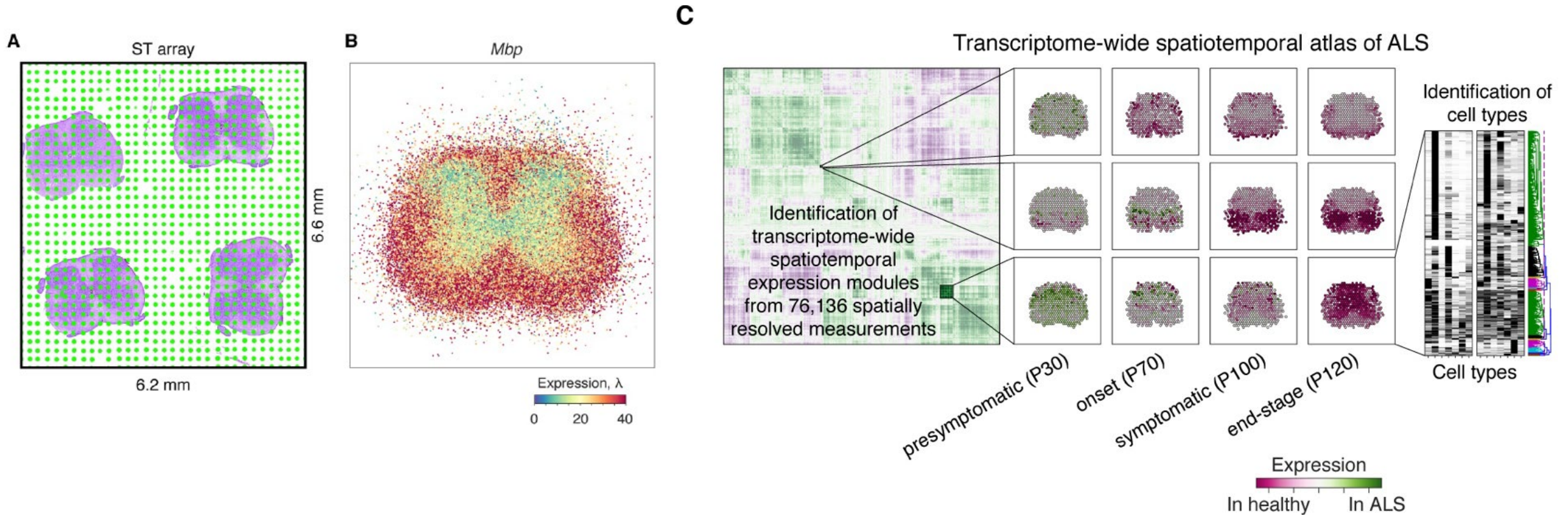
## WHAT THEY DID

- Time course ST on mouse spinal cord tissue and post mortem ALS patients' tissue
- Description of regional and temporal differences in microglia and astrocytic populations
- Analysis of changes in transcriptional pathways shared between mouse and ALS patients.

## HOW THEY DID IT

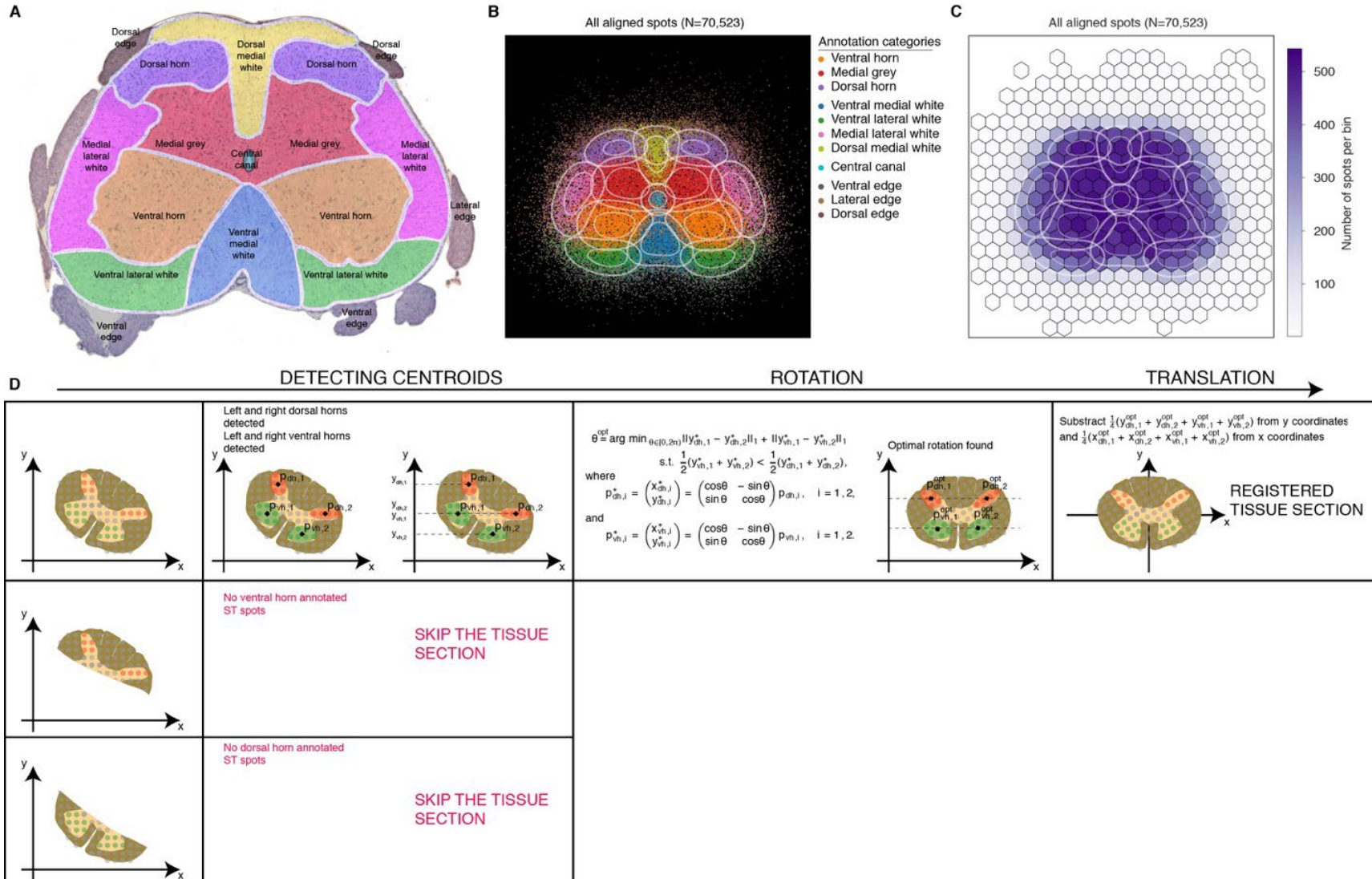
- They compared SOD1-G93A (ALS) mouse to controls SOD1-WT at pre symptomatic, onset, symptomatic and end-points stages for a total of 67 mice and ~1200 tissue sections
- Plus 80 post mortem sections from ALS patients

# Analytical workflow to determine expression modules across samples



- Identification of coordinated expression modules across several cell types
- Focus on how these expression modules change across time, between genotypes and within specific cells types.

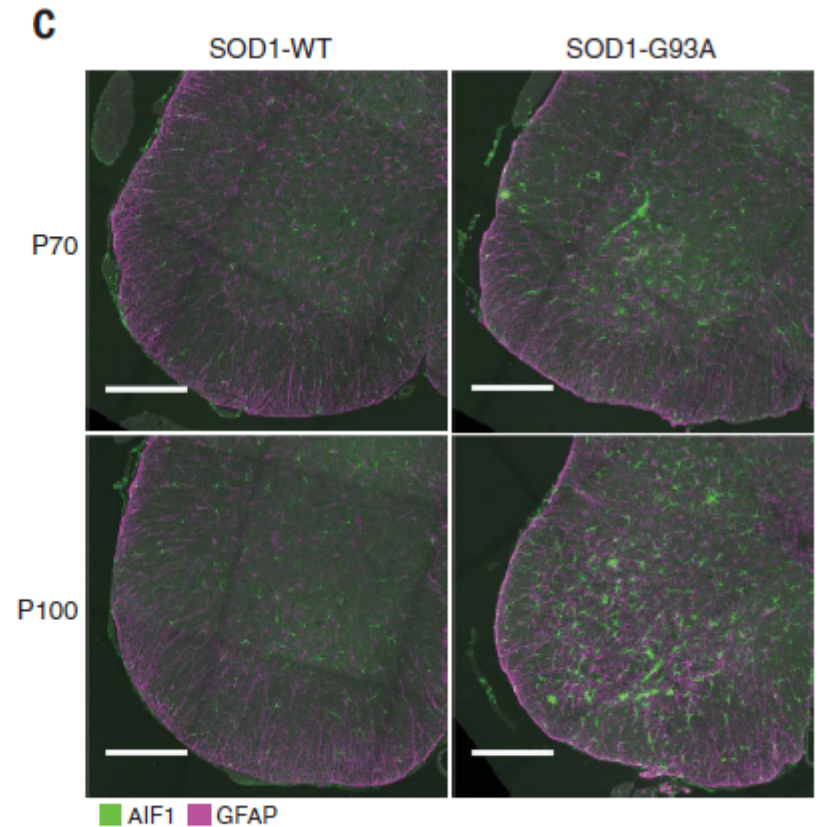
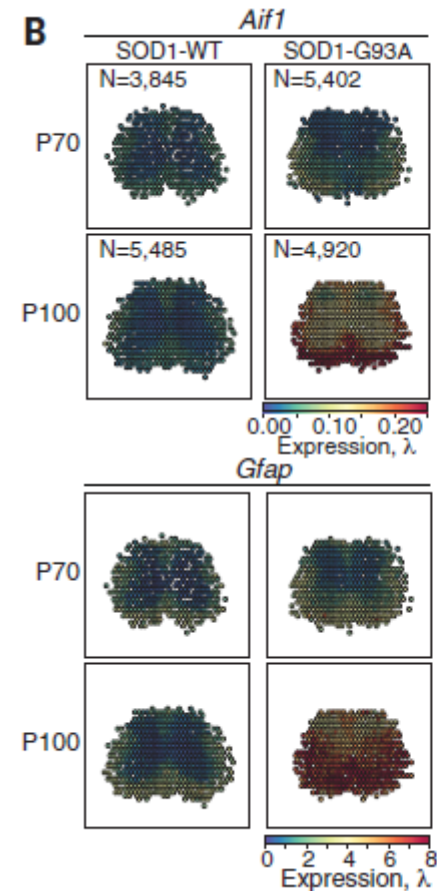
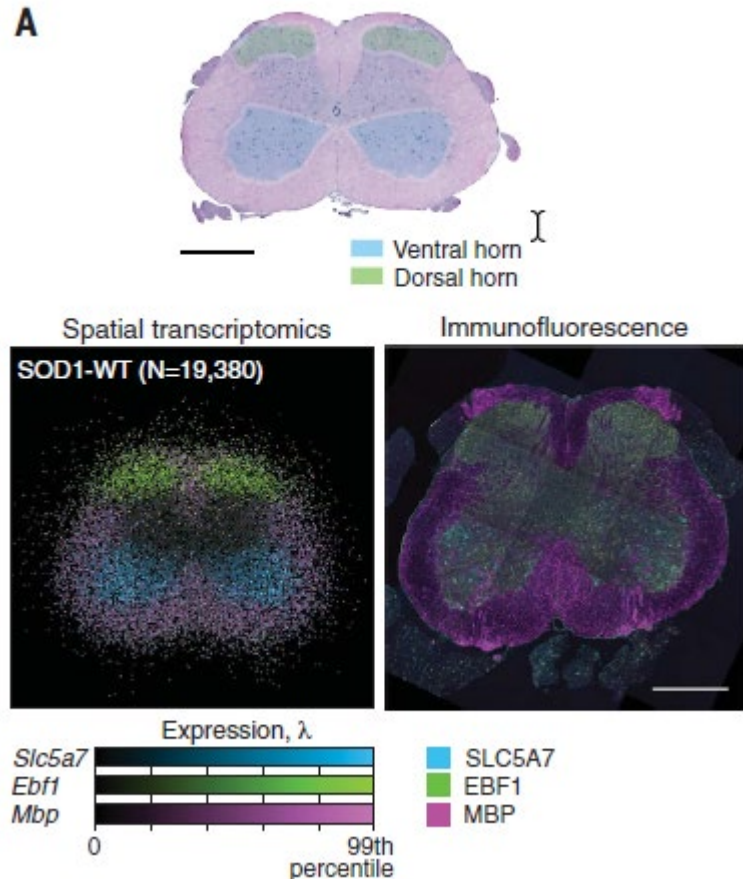
# Spatial arrangement of ST spots



- Anatomical annotation regions (AARs) to assign mouse ST spots to specific anatomical areas

- Tissue sections are then aligned to the established AARs, rotating the tissue when needed so that the discrepancies between left and right dorsal and ventral horns are minimized

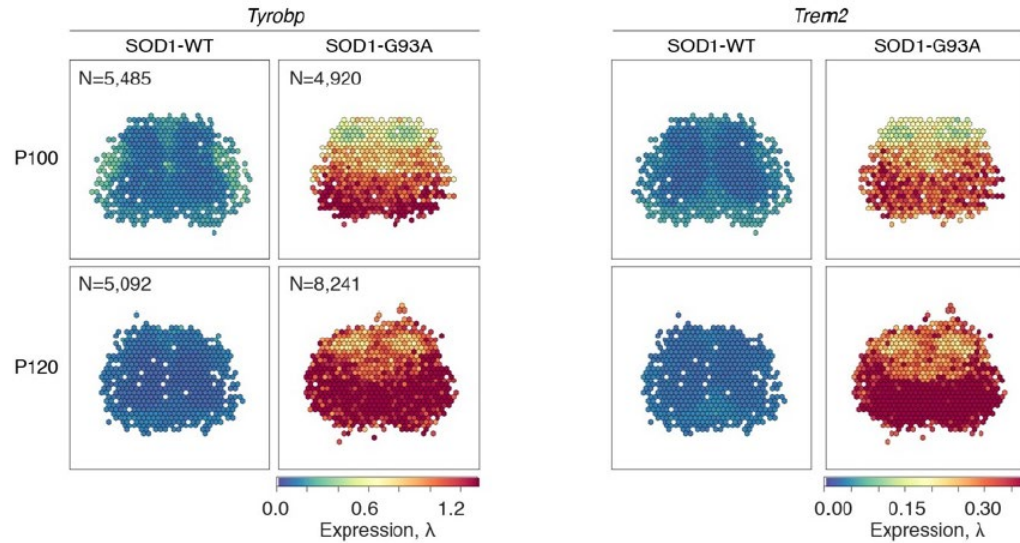
# ST vs immunohistochemistry



→ Spatial concordance between immunofluorescence and analysed mRNA levels

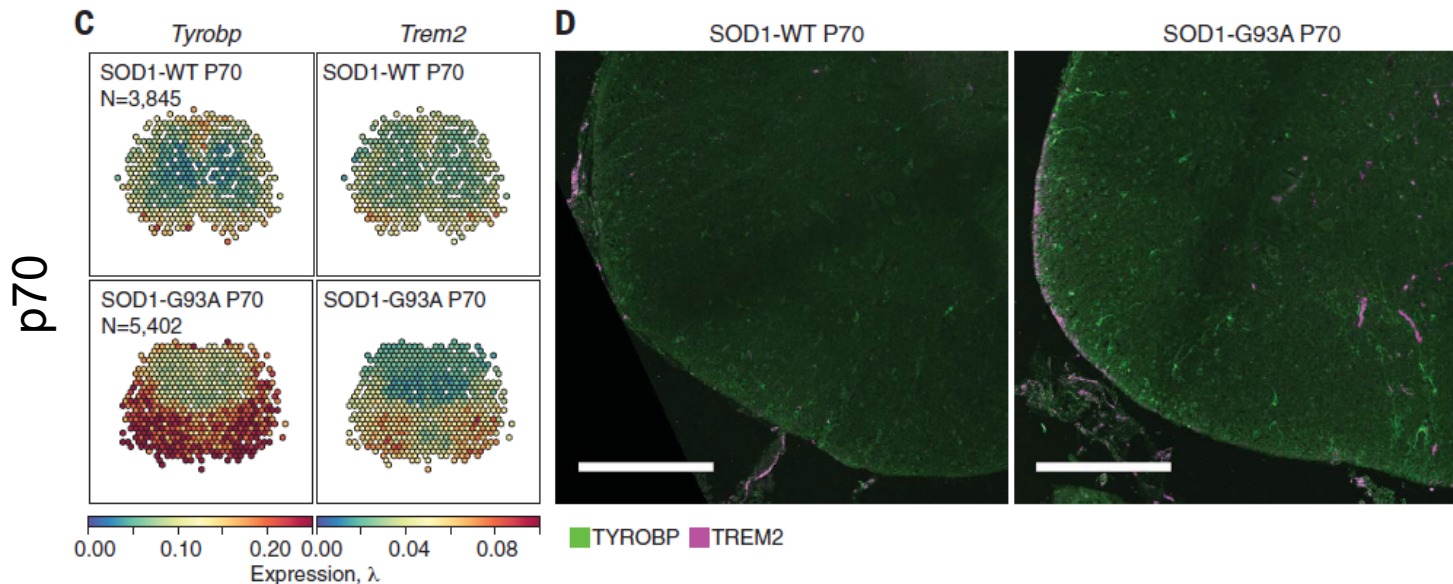
→ Markers of microglia (*Aif1*) and astrocytes (*GFAP*) are elevated at the symptomatic stage

# Pre-symptomatic dysregulation of TREM2- and TYROBP mediated signalling



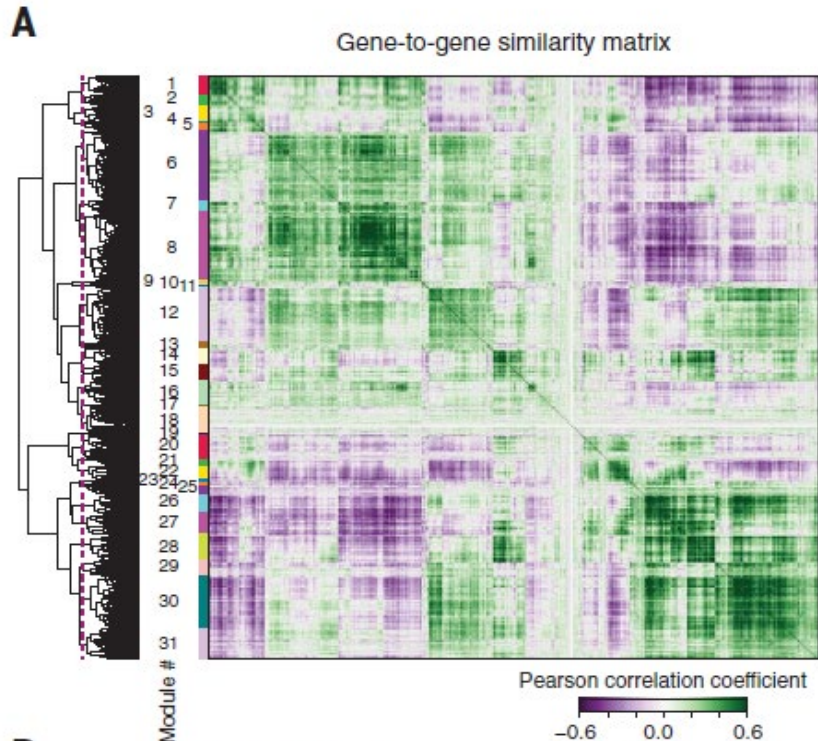
Use of TREM2, often reported in other neurodegenerative diseases (AD, ALS, MS):

→ TREM2 and TYROBP form a receptor complex that can trigger phagocytosis or modulate cytokine signalling



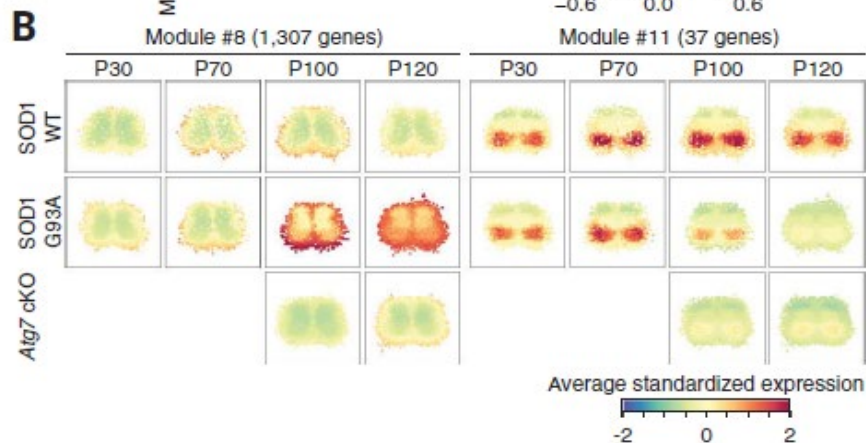
→ *Tyrobp* expression is up-regulated pre symptomatically and before *Trem2* in the ventral horn and ventral white matter

# Use of co-expression modules changes in space and time of pathways activities

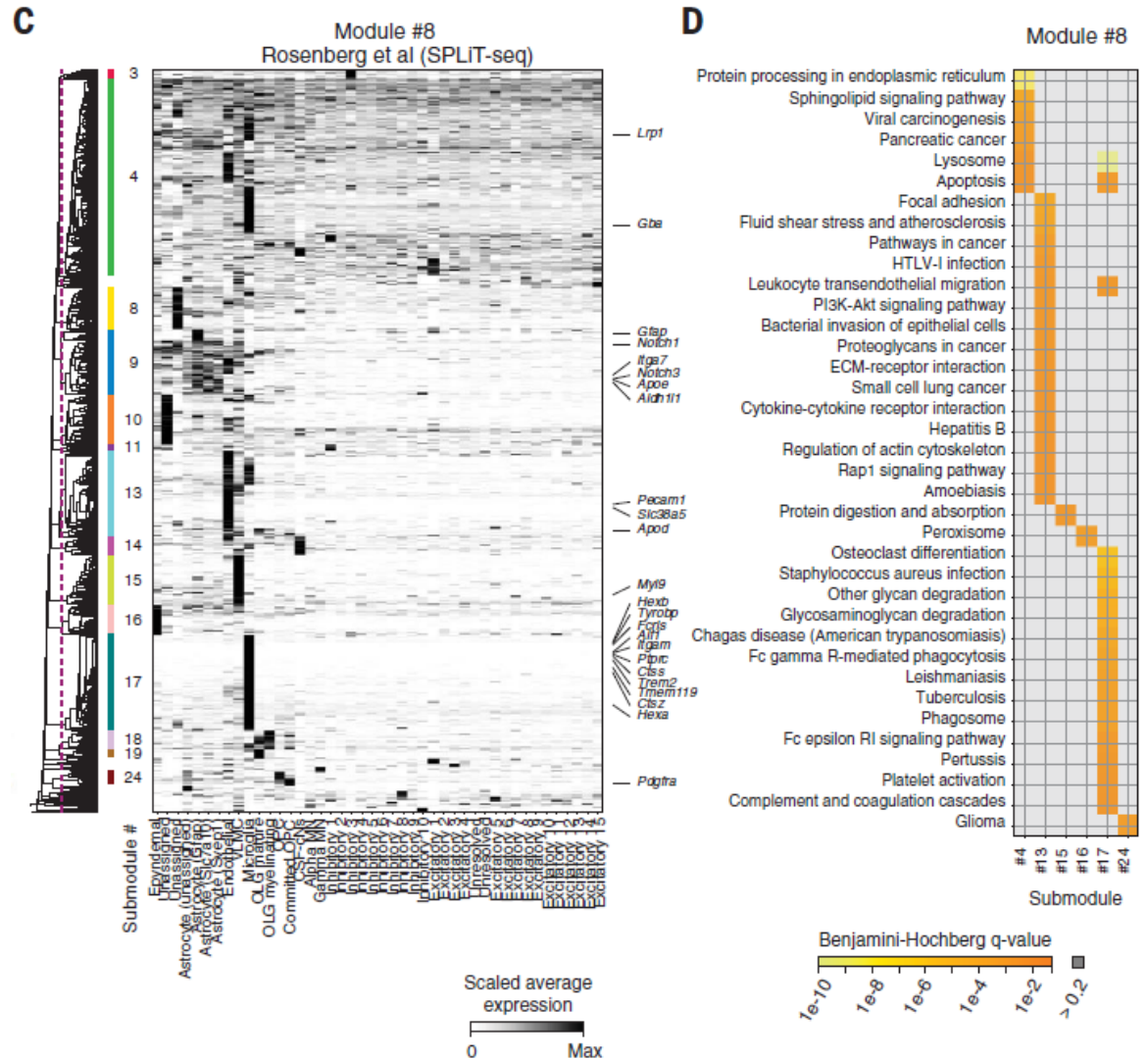


→ 31 co-expression modules by clustering mouse SGEMs

- *Trem2* expression modulates autophagy in myeloid cells.
  - Mutation of several autophagy genes are associated to ALS.
  - Ablation of autophagy by conditional knockout of *Atg7* in cholinergic cells, including motor neurons leads to earlier symptom onset but prolonged survival in ALS mice
- Some of those modules are affected by *Atg7* cKO.



# Division of modules into submodules by cell-type-specific expression patterns



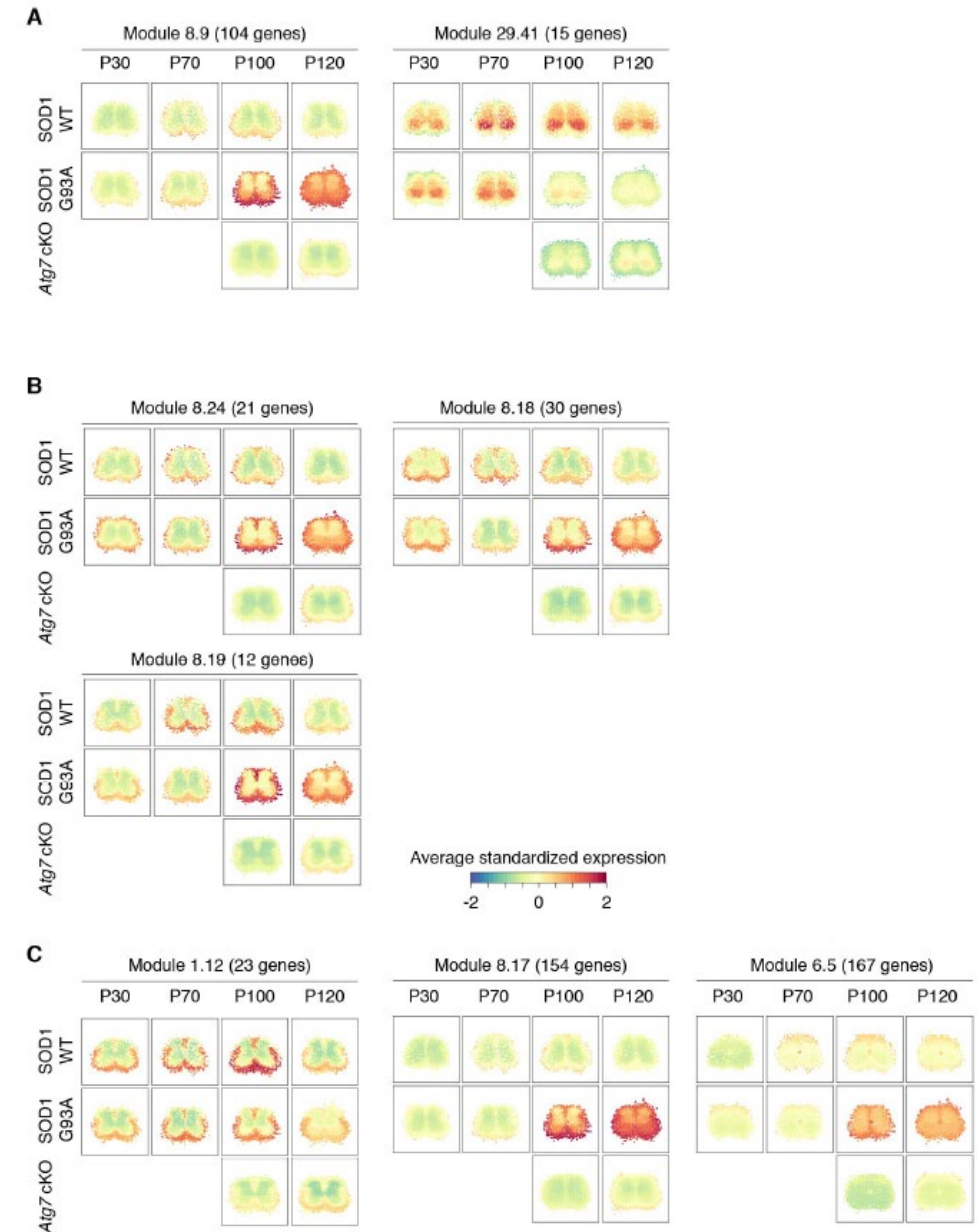
- Submodules that are enriched for a given cell type can display distinct spatiotemporal expression patterns
- Hierarchical clustering of genes in module 8 using independent gene expression data of mouse central nervous system cell types.
- Such differences represent functionally distinct subpopulations within that cell type
- Analysis of enriched pathways among the genes for submodules in module 8

# Regional glial expression submodules

Astrocytes behaving differently based on gene expression and spatial distribution

Oligodendrocyte precursor cells (8.24), mature OLG (8.18), and mature/myelinating OLG (8.19)

Microglia's submodule 8 activity is correlated to astrocytes and OLG submodules



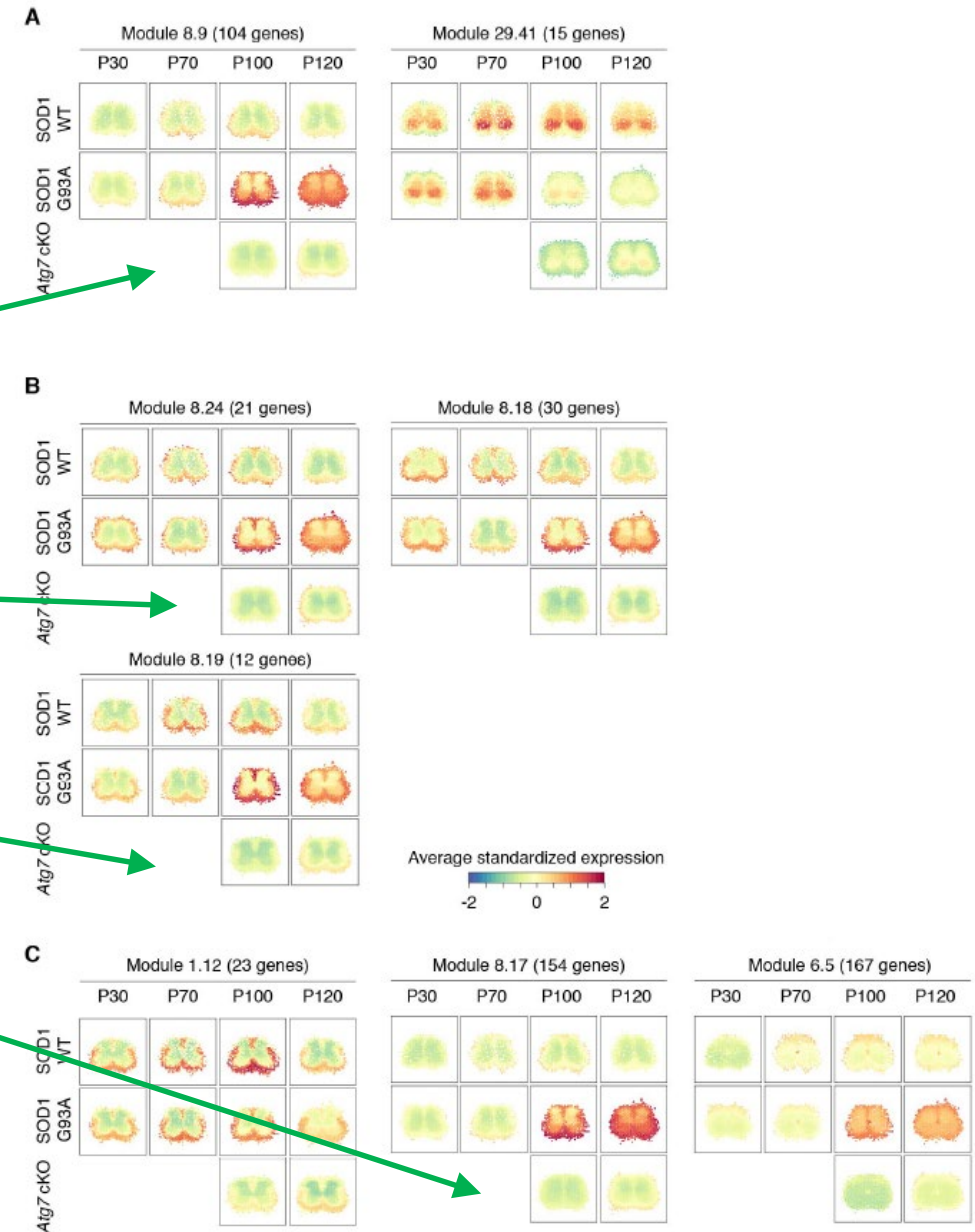
# Regional glial expression submodules

The spatiotemporal pattern of module 8 expression is rescued by ablation of autophagy in cholinergic neurons in Atg7 cKO mice

Astrocytes behaving differently based on gene expression and spatial distribution

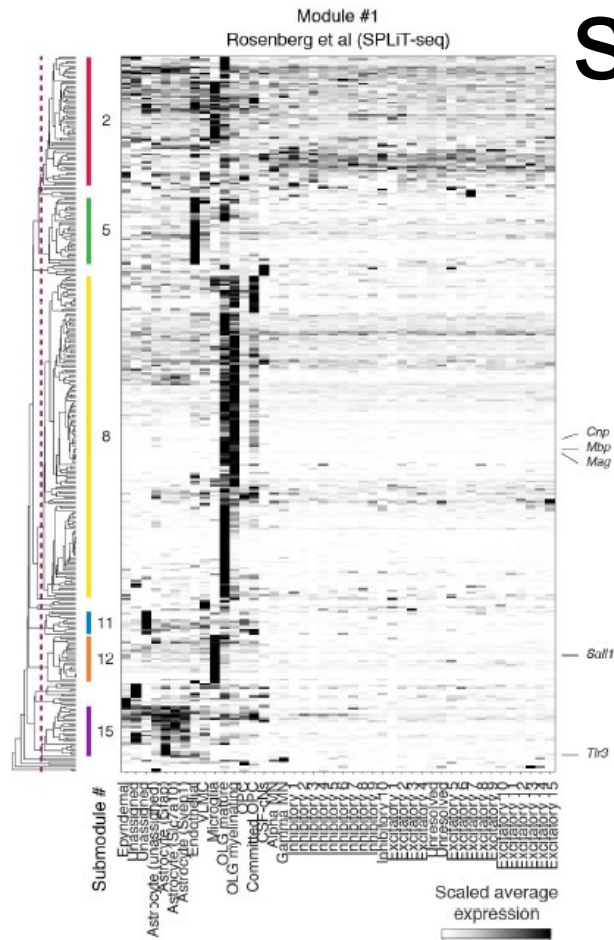
Oligodendrocyte precursor cells (8.24), mature OLG (8.18), and mature/myelinating OLG (8.19)

Microglia's submodules activity is correlated to astrocytes and OLG submodules

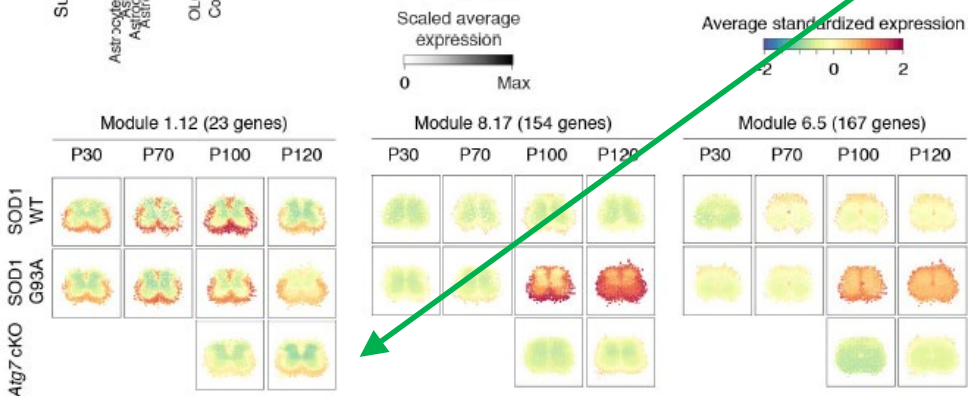




# Digging into microglia expression of submodules across modules

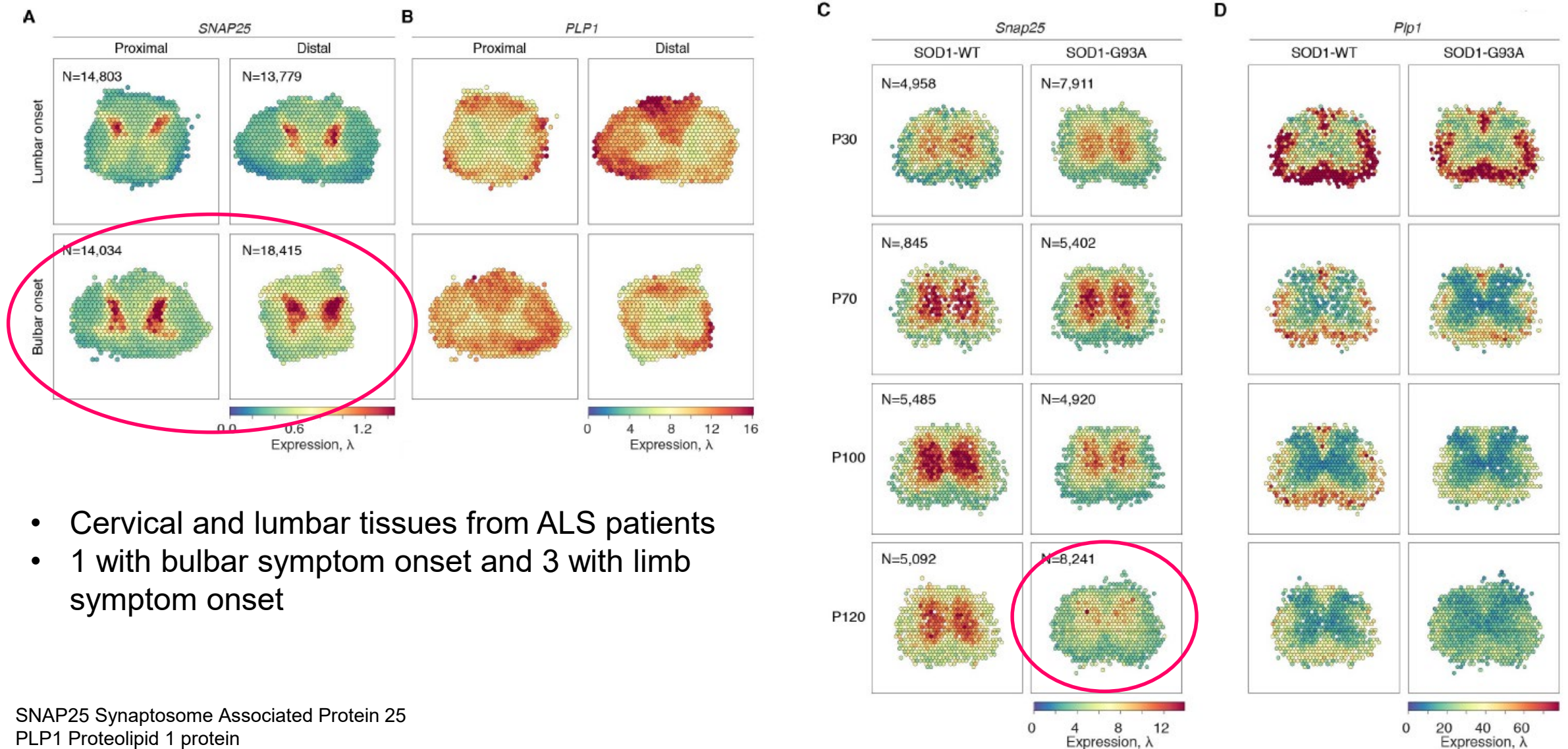


- Microglia submodule 1.12 includes *Sall1*
- *Sall1* is expressed by homeostatic microglia, and loss of *Sall1* expression results in a phagocytic, inflammatory phenotype
- The expression pattern of the *Sall1* submodule illustrates glial interactions that are spatiotemporally and mechanistically distinct from those of module 8 and 6
- *Atg7* cKO does not rescue the dynamics of this expression module





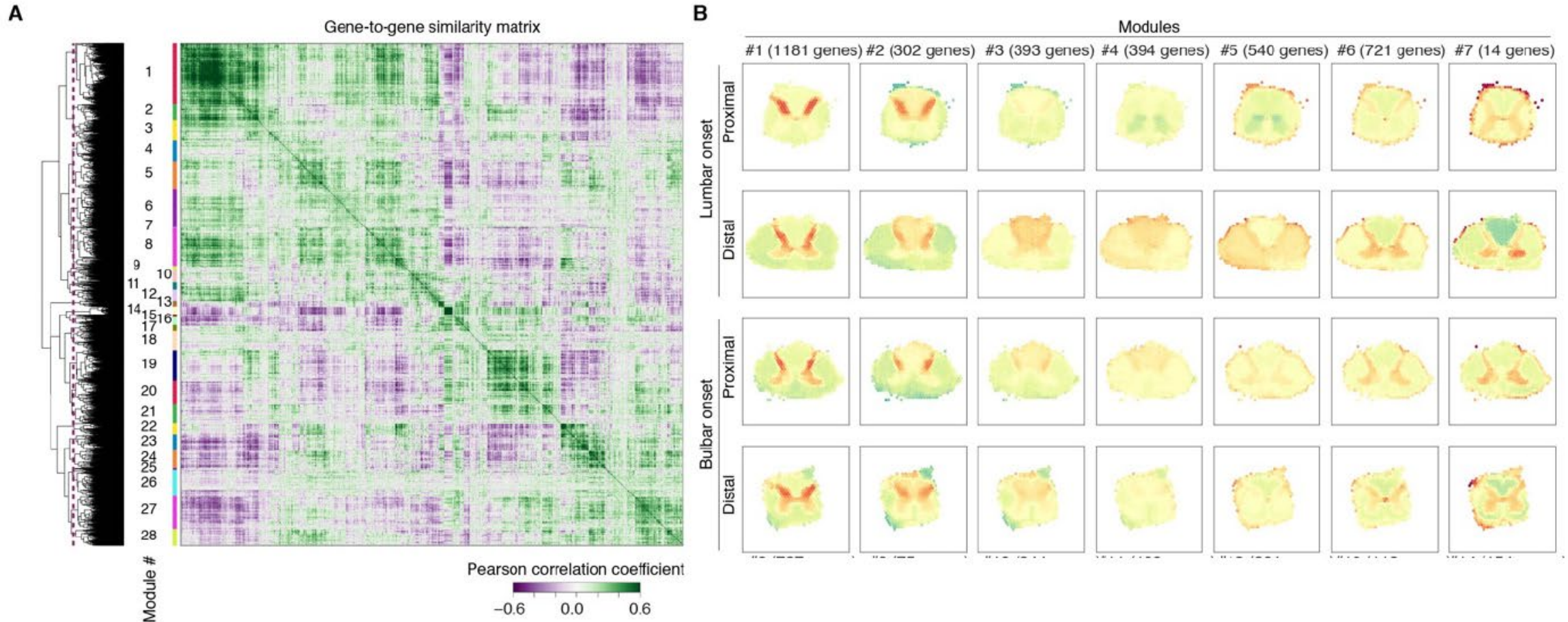
# Similarity of regional expression patterns between patients and mice



- Cervical and lumbar tissues from ALS patients
- 1 with bulbar symptom onset and 3 with limb symptom onset

→ SNAP25 Synaptosome Associated Protein 25  
 → PLP1 Proteolipid 1 protein

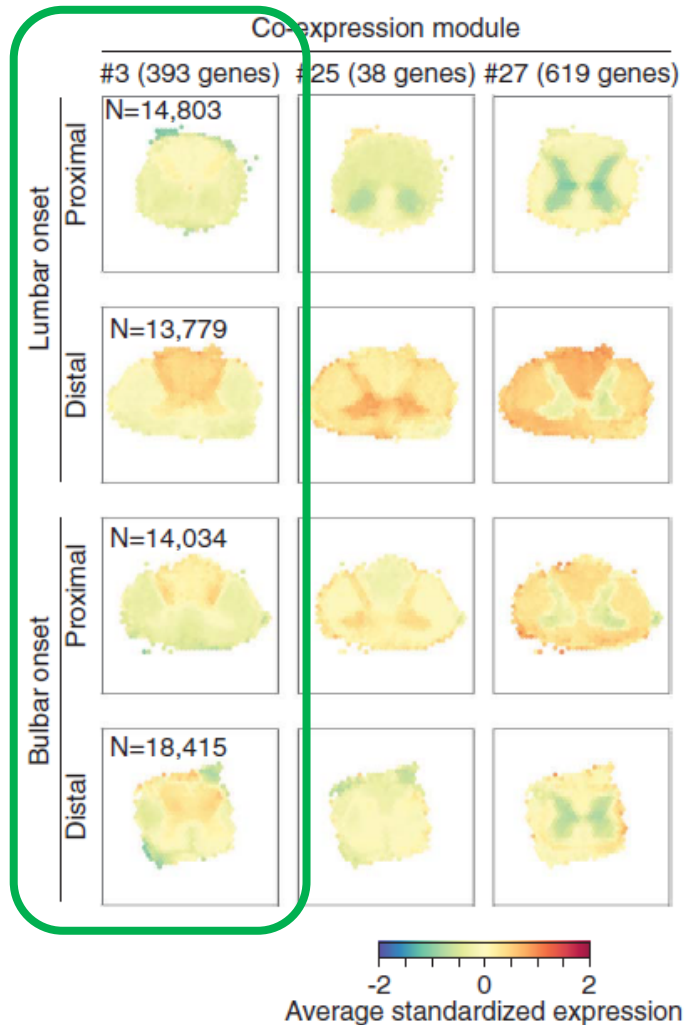
# Unbiased co-expression analysis to find expression modules on human samples



→ Anatomical annotation regions (AARs) characteristic expression patterns

→ Differences between white and grey matter (as well as dorsal vs ventral)

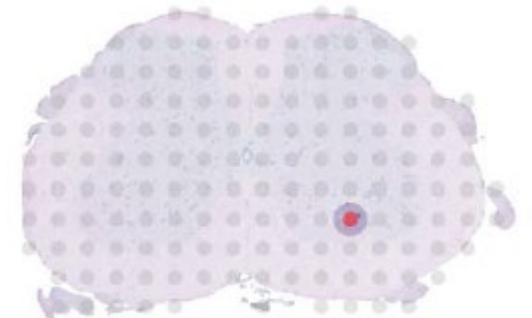
# Unbiased co-expression analysis to find expression modules on human samples



- Pathway enrichment analysis showed module 3 is enriched for sphingolipid pathways
  - Altered sphingolipid levels and metabolism have been reported in spinal cord of ALS mouse models and patients
  - Modulators of sphingolipid signalling have been proposed as possible therapeutics
- This data show details dynamics in sphingolipid signalling in multiple cell types

# ALS paper summary

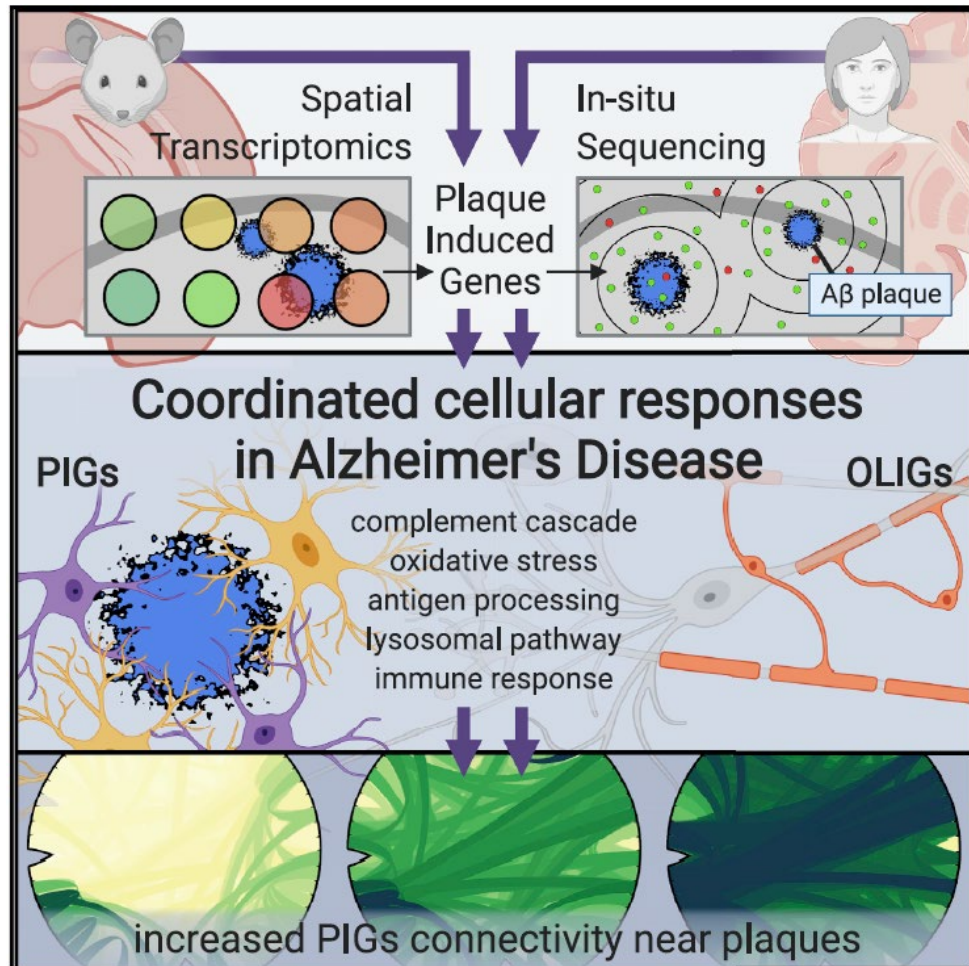
- Spatiotemporal and transcriptome-wide gene expression data combining resolution, replication and biological perturbation
  - Analysis of glial cells behaviour based on their spatial location and disease time points
  - Identification of mechanisms that can rescue the glial phenotype based on the time point (e.g. autophagy)
- Allows comparisons and correlations between mouse models and patients samples
- Offers potential new therapeutics targets when describing perturbed pathways (e.g. sphingolipids)



# Spatial transcriptomics and *In Situ* sequencing to study Alzheimer's disease

Chen et al., *Cell* **182**, 976-991 (2020)

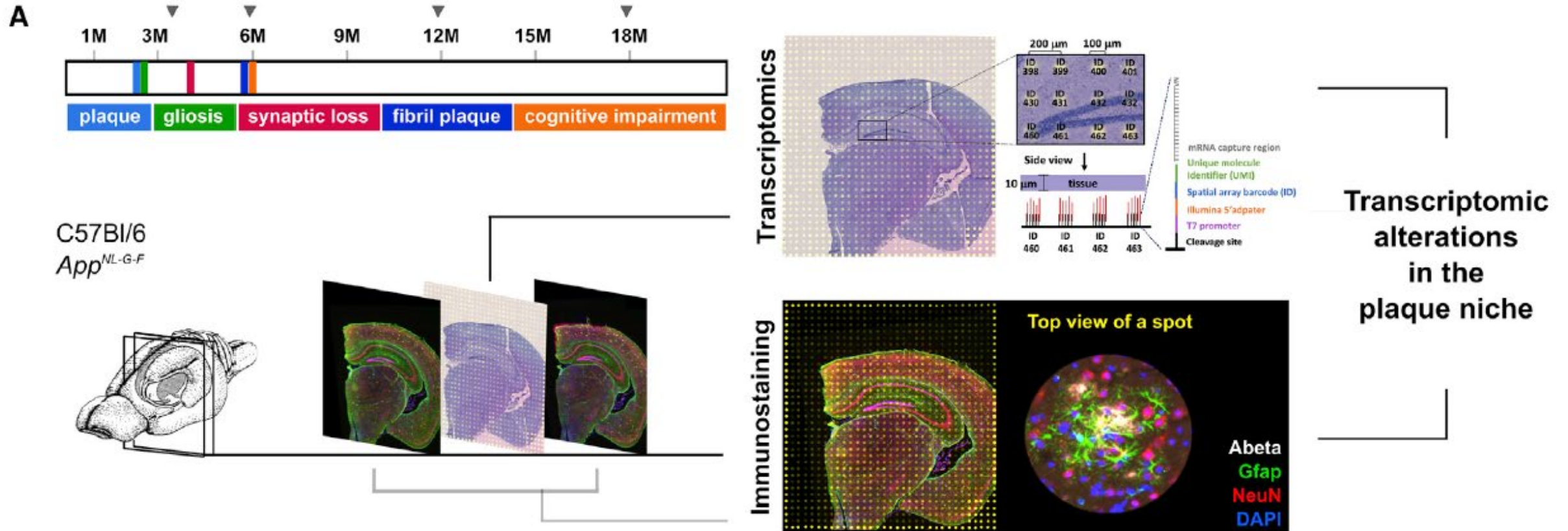
## WHAT THEY DID



## HOW THEY DID IT

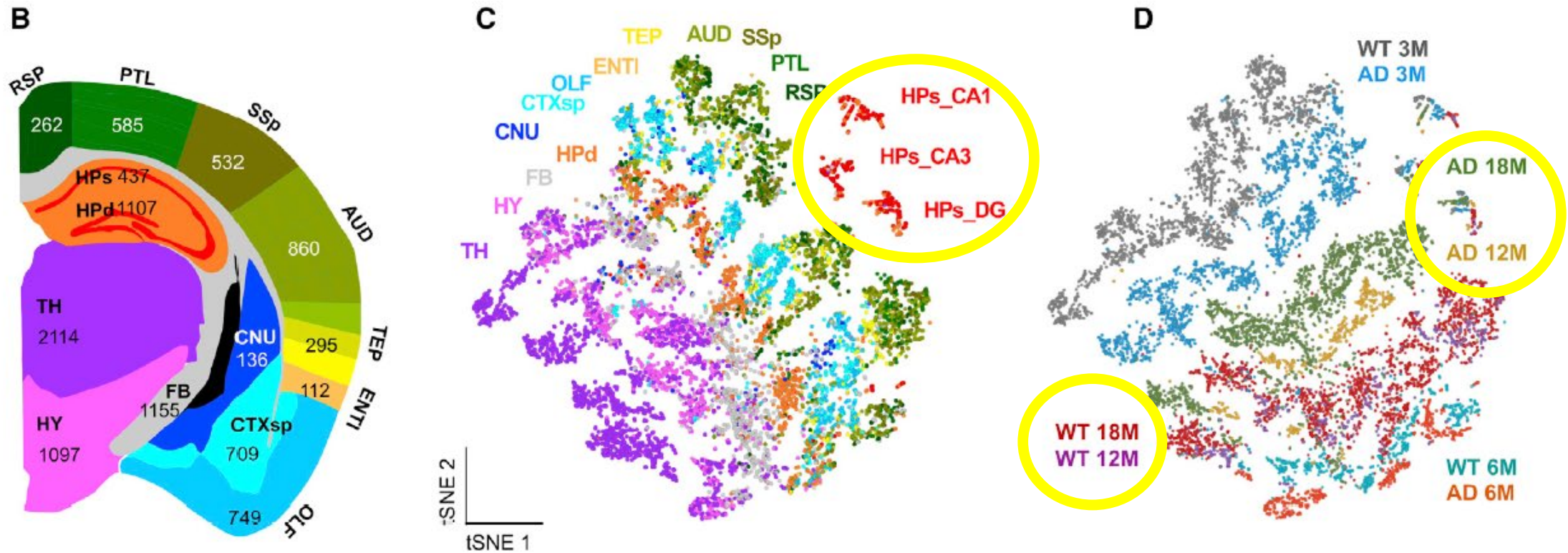
- Transcriptome-wide analysis in hundreds of 100  $\mu\text{m}$  diameter around amyloid plaques
- Addition of *in situ* sequencing of selected transcript for single cell resolution (Qian et al. 2020)
- Analysis on AppNL-G-F mice and human samples

# Experimental set up to match ST data with protein stain



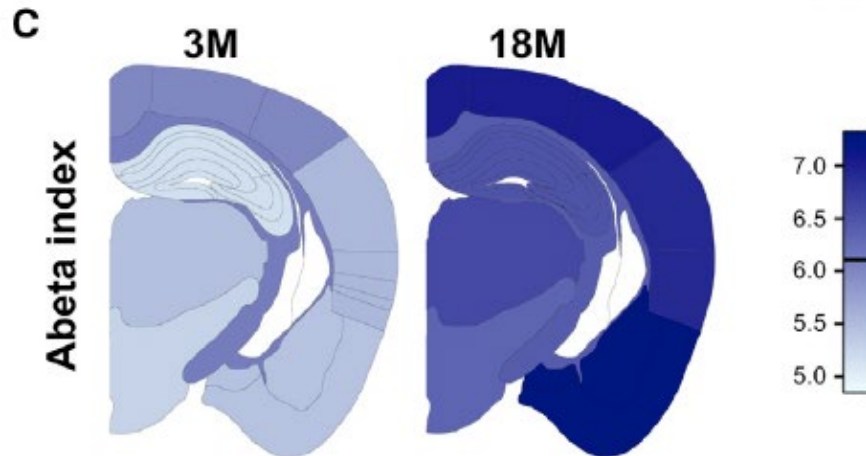
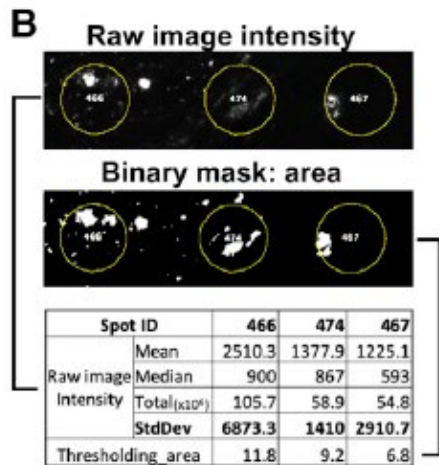
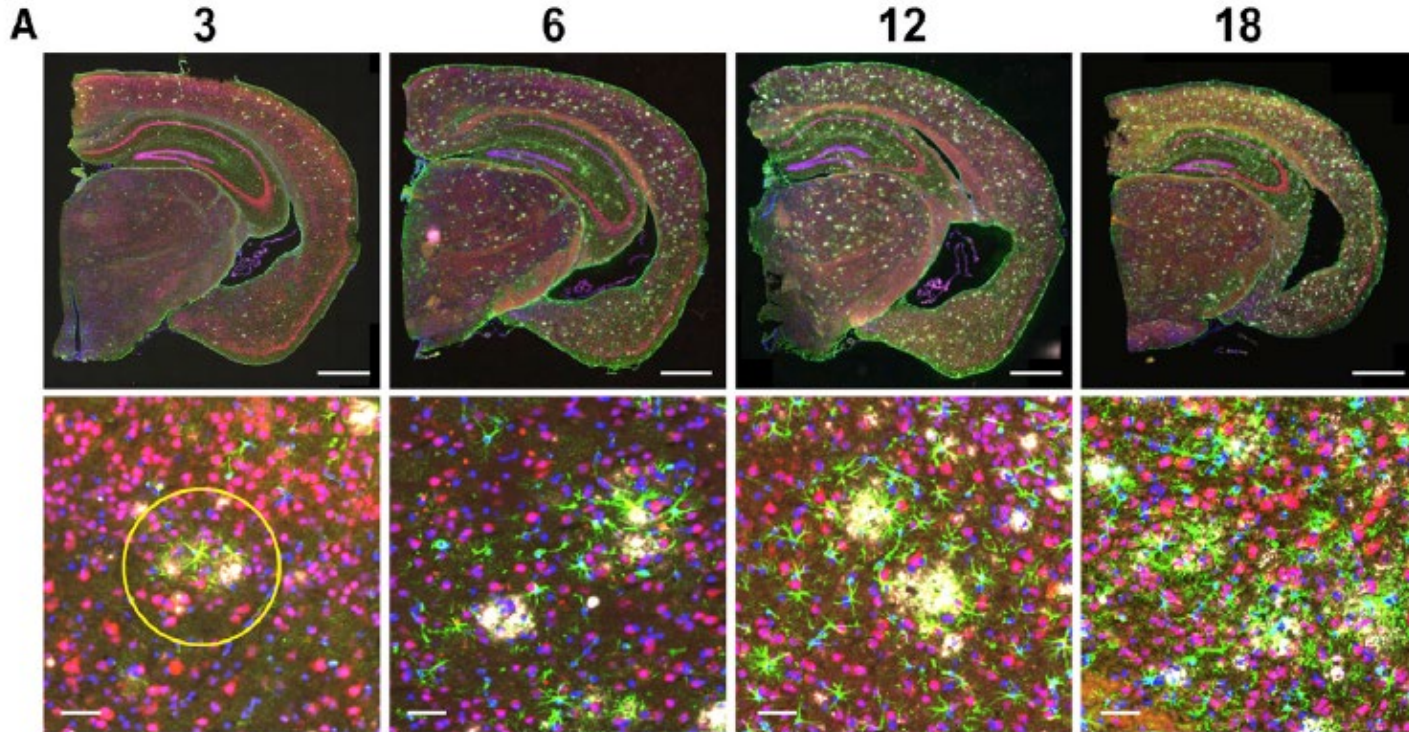
- Every coronal section contained more than 500 transcriptomics profiles of individual TDs, adding up to 10,327 transcriptomics profiles over 20 coronal sections
- Each TD was annotated with spatial, pathological and cellular annotation and the aligned with staining for A $\beta$ , reactive astrocytes, neurons and DAPI.

# Clustering of transcriptomic profiles by brain region and genotype



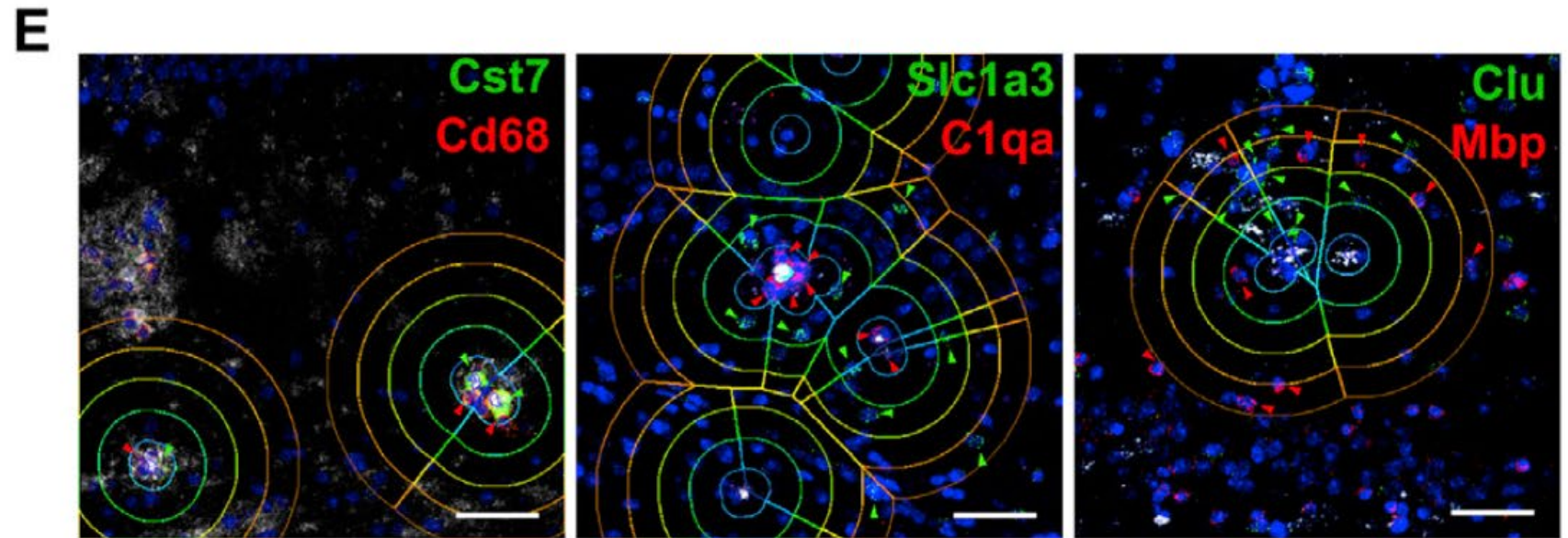
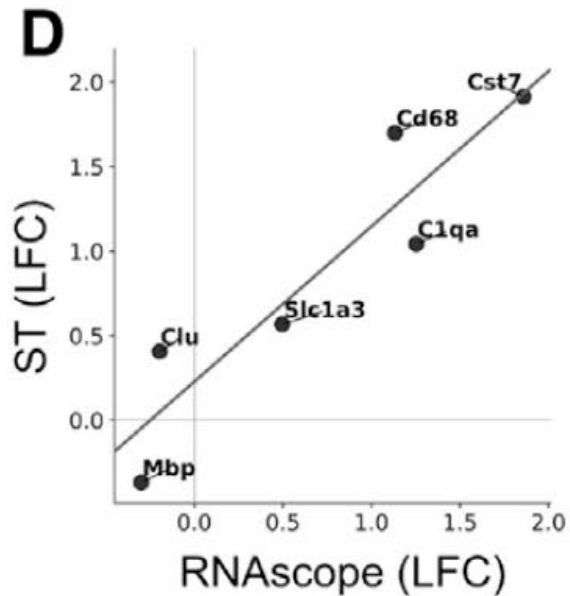
- Every coronal section was then aligned to the Allan Mouse Brain Atlas and each TD was assigned to a specific brain region
- The 10,327 transcriptomic profiles clustered according to brain regions and also according to age and phenotype of the animals

# Defining A $\beta$ load for altered gene expression analysis



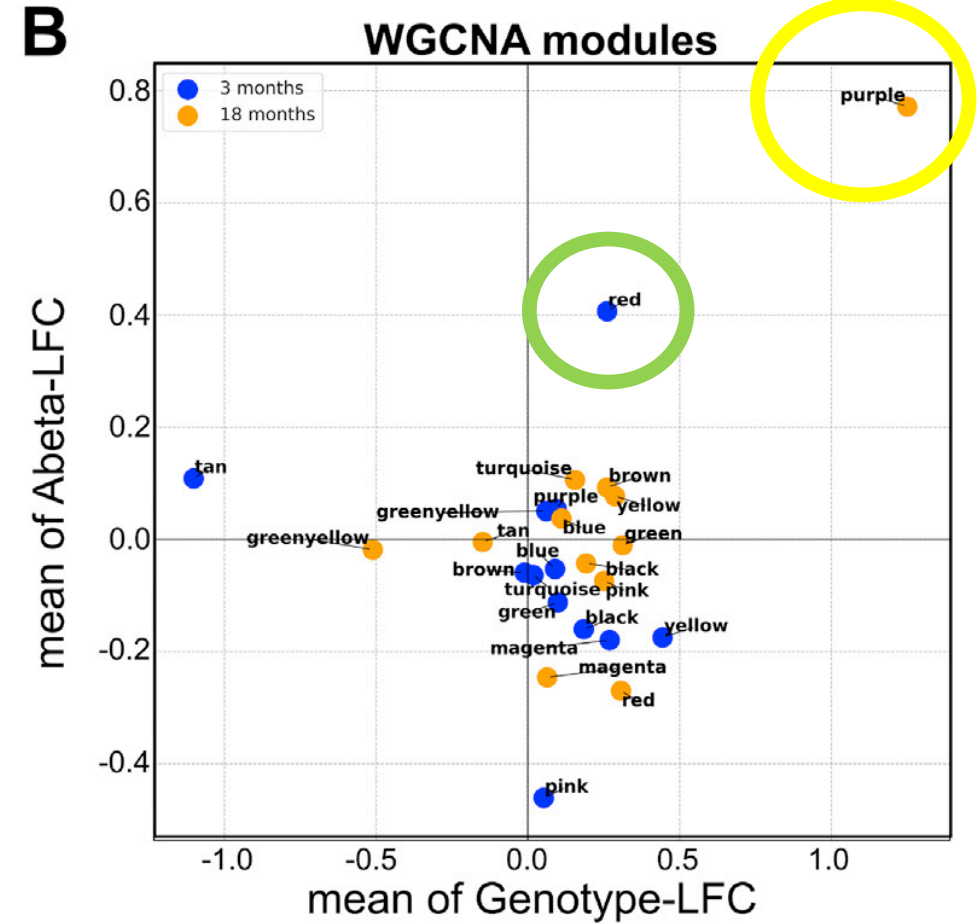
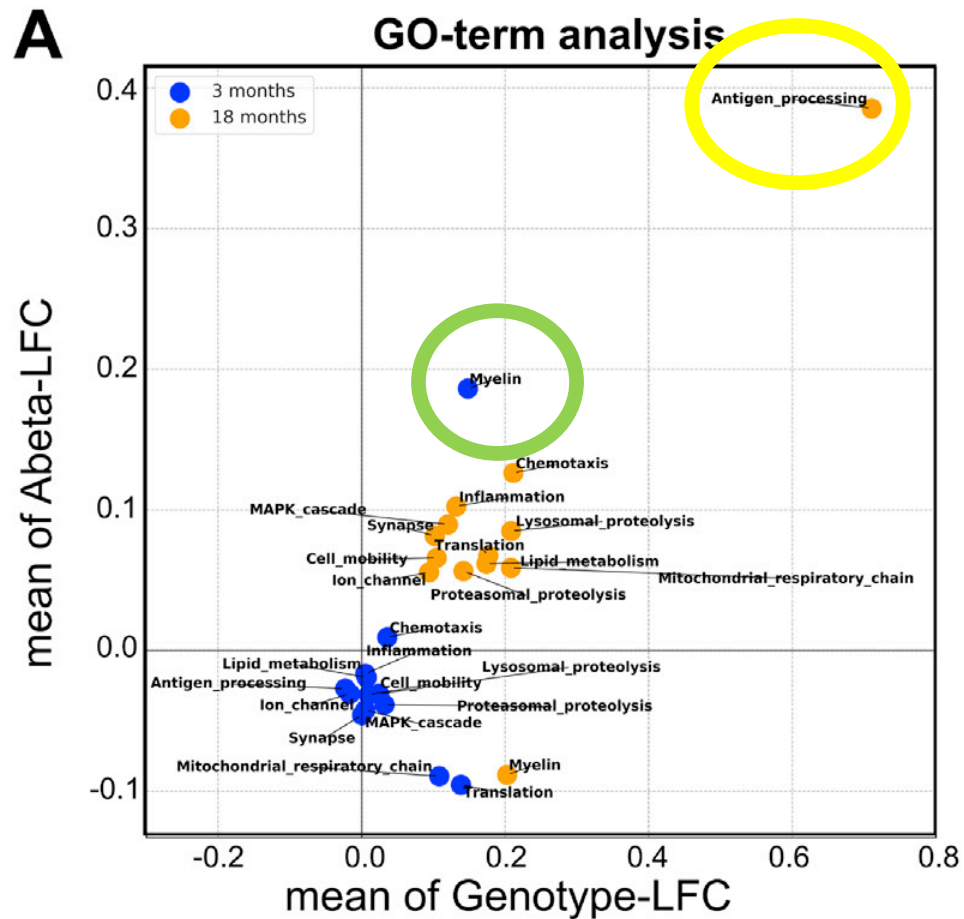
- Use of standard deviation of A $\beta$  fluorescence intensity pixels in TD as A $\beta$  index
- That separates mild from high A $\beta$  accumulation
- You can average the A $\beta$  index for each TD per brain region and match it with immunostaining results

# Validation of ST on A $\beta$ model using RNAscope



- Analysis of 6 transcripts by RNAscope known to be dysregulated in App<sup>NL-G-F</sup> mice at 18 months of age
  - Grouped the cells in 5 concentric rings around the plaques
  - Measure mean intensity of hybridization in ring 1 (close to plaque) vs ring 5 (far from plaque)
- Log fold change (LFC) of gene expression detected with RNA scopes correlates to LFC obtained with ST

# Expression analysis based on A $\beta$ load or on genotype

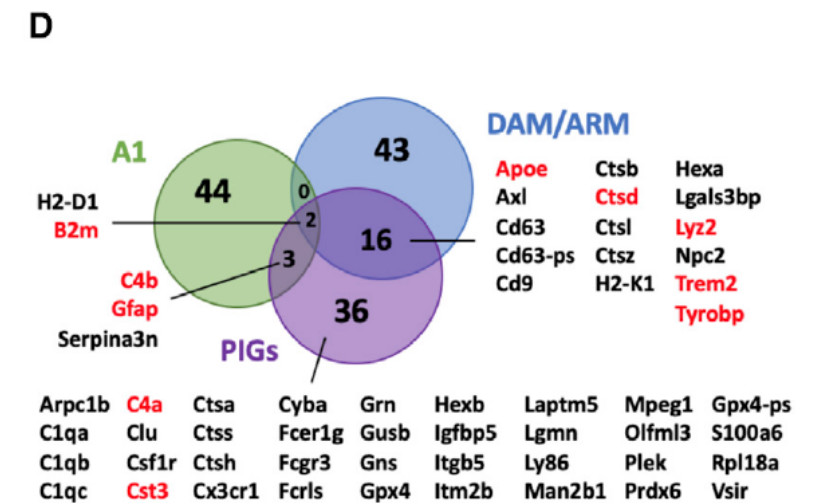
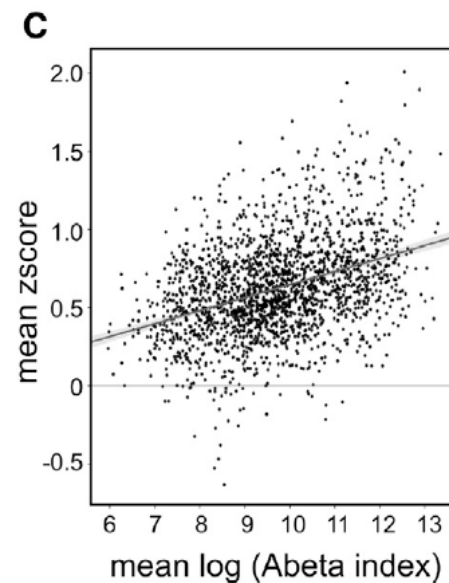
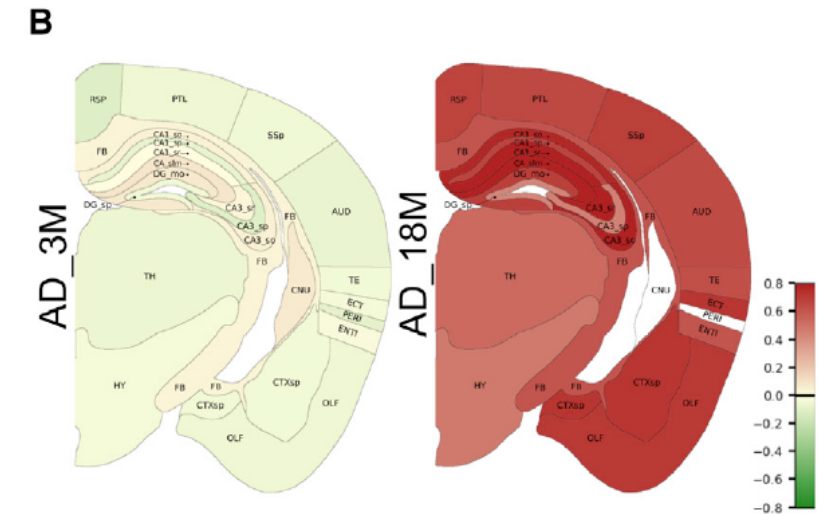
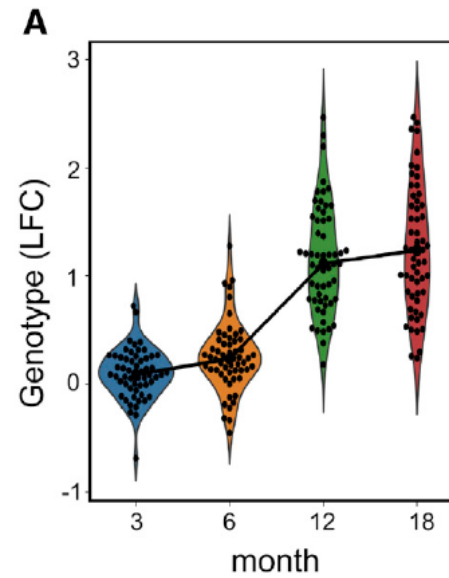


- Use of a gene ontology platform on genes ranked according to the LFC on the genotype axis and on the A $\beta$  axis to identify 13 super-categories

- Grouping 50% of most variably expressed genes based on similar expression patterns to find 12 separate modules

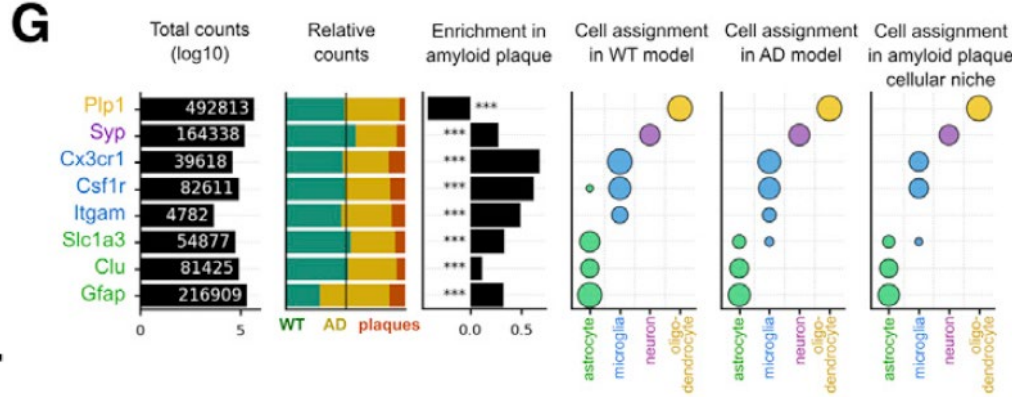
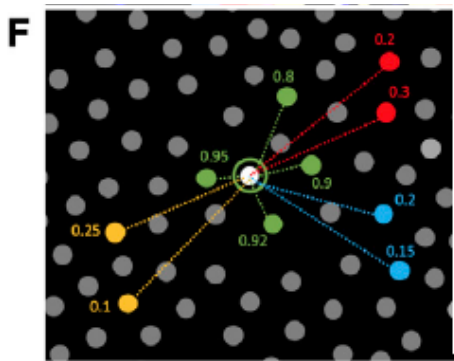
# Identification of plaque induced genes (PIGs)

- Purple module includes 57 genes, defined as Plaque Induced Genes (PIGs)
- This module increases expression over 6-12 months to then have an whole brain response
- There is a correlation between A $\beta$  accumulation and PIG expression across all TD
- The cellular signature of the PIG module has a strong association with activated microglia (DAM/ARM) and with inflammatory astrocytes

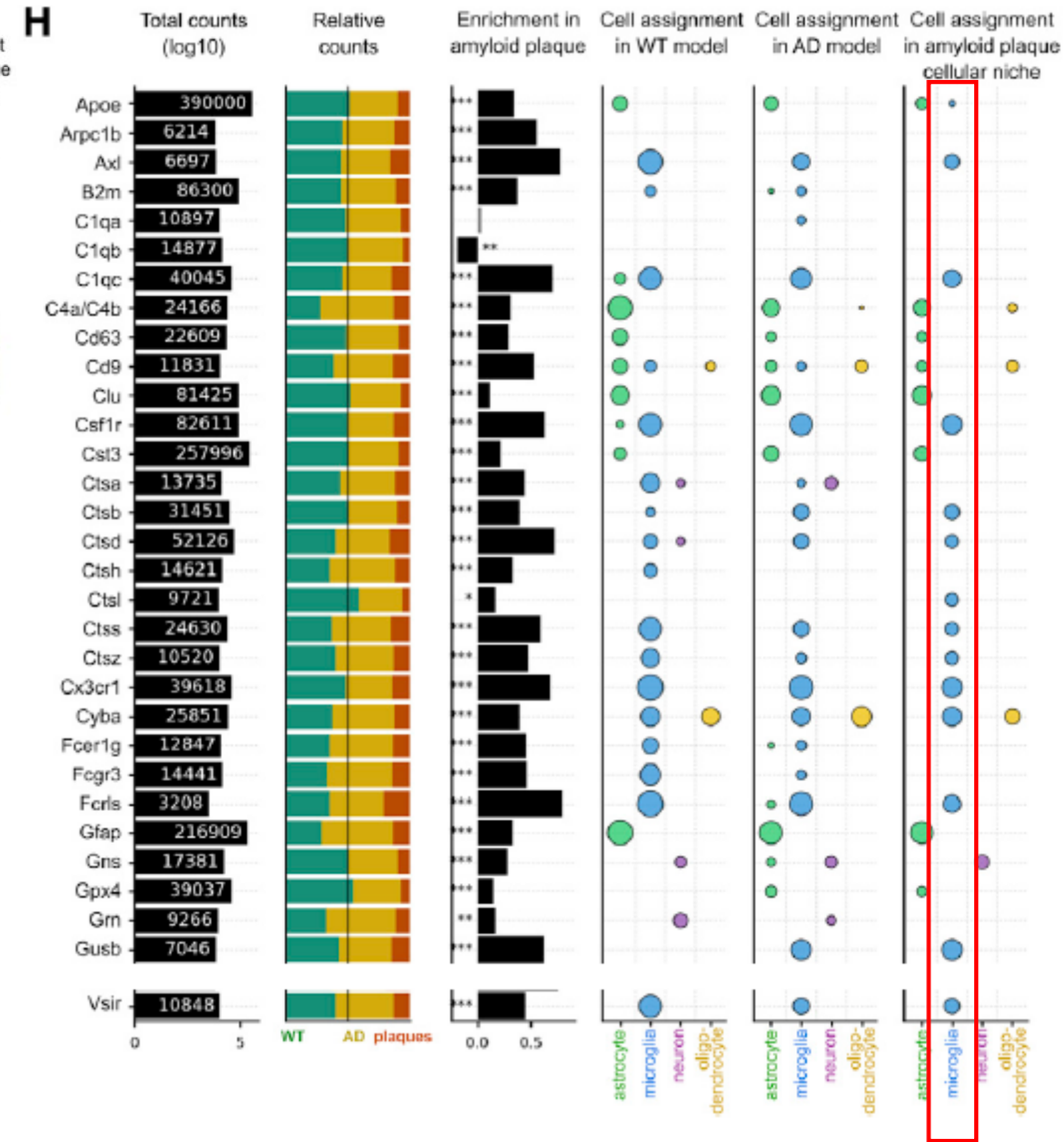




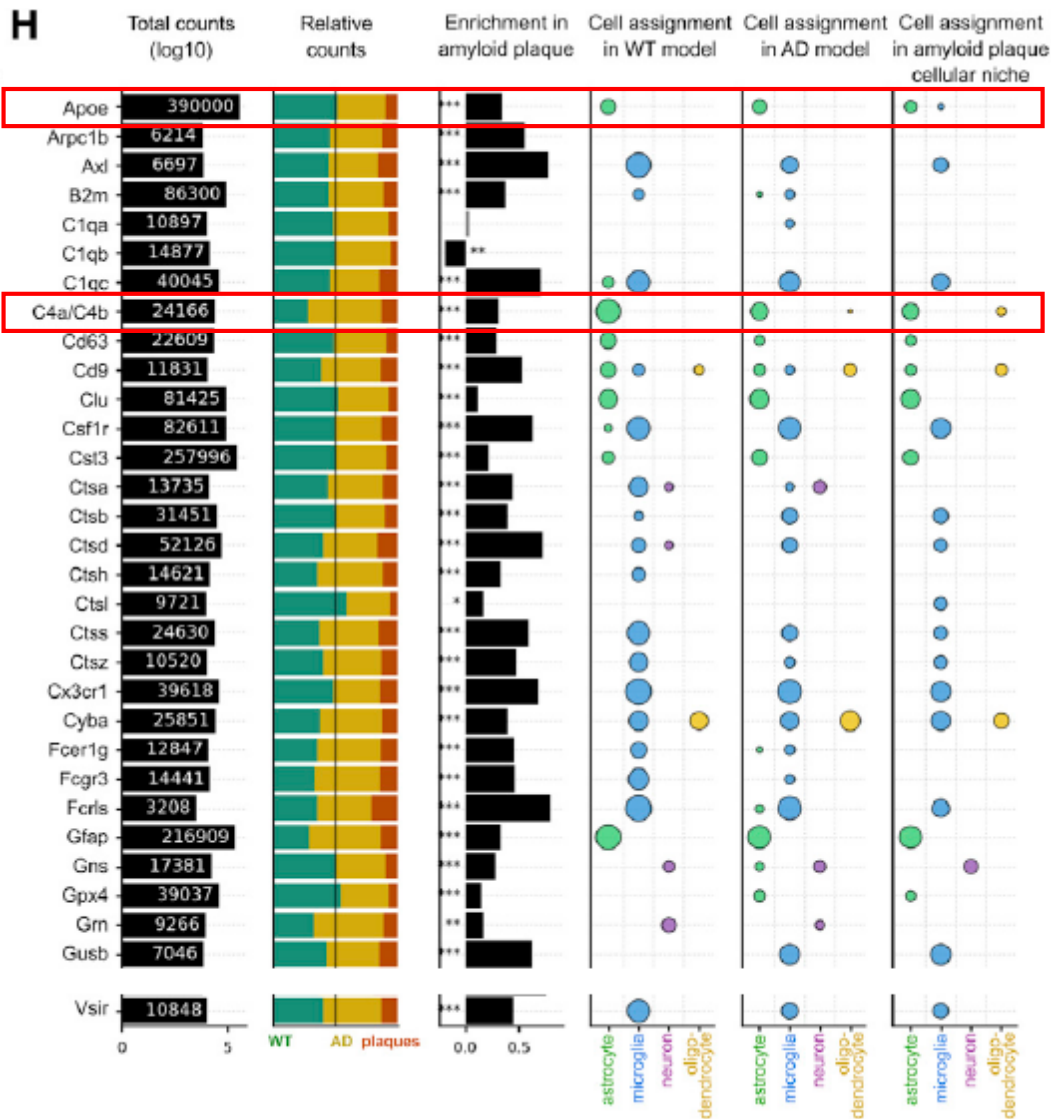
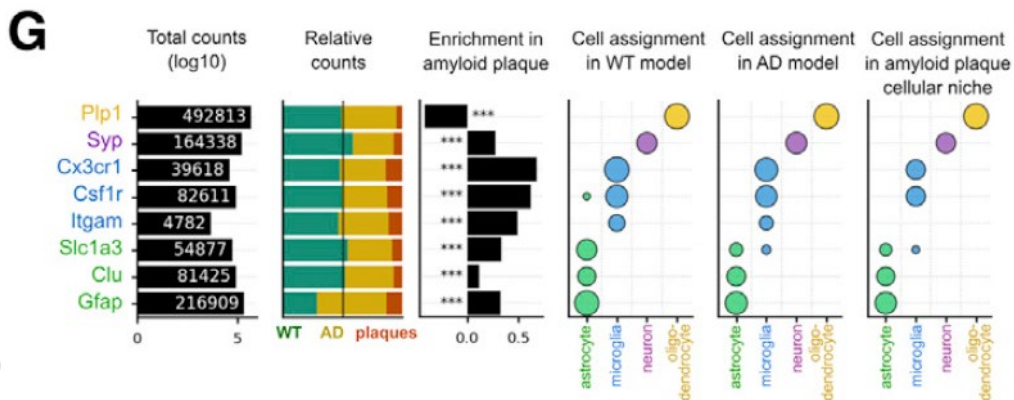
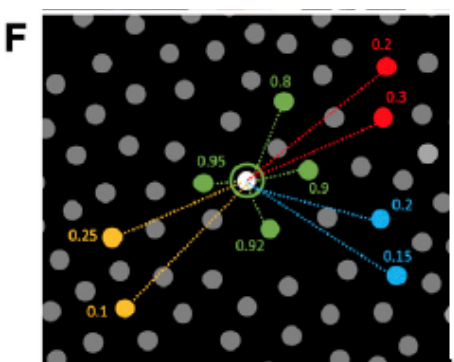
# Cellular signature of PIGs by ISS



- Each punctum is assigned to a cell type by calculating the enrichment in cell-type marker puncta within its 5 um radius
- PIG response to plaque is largely contributed by microglia



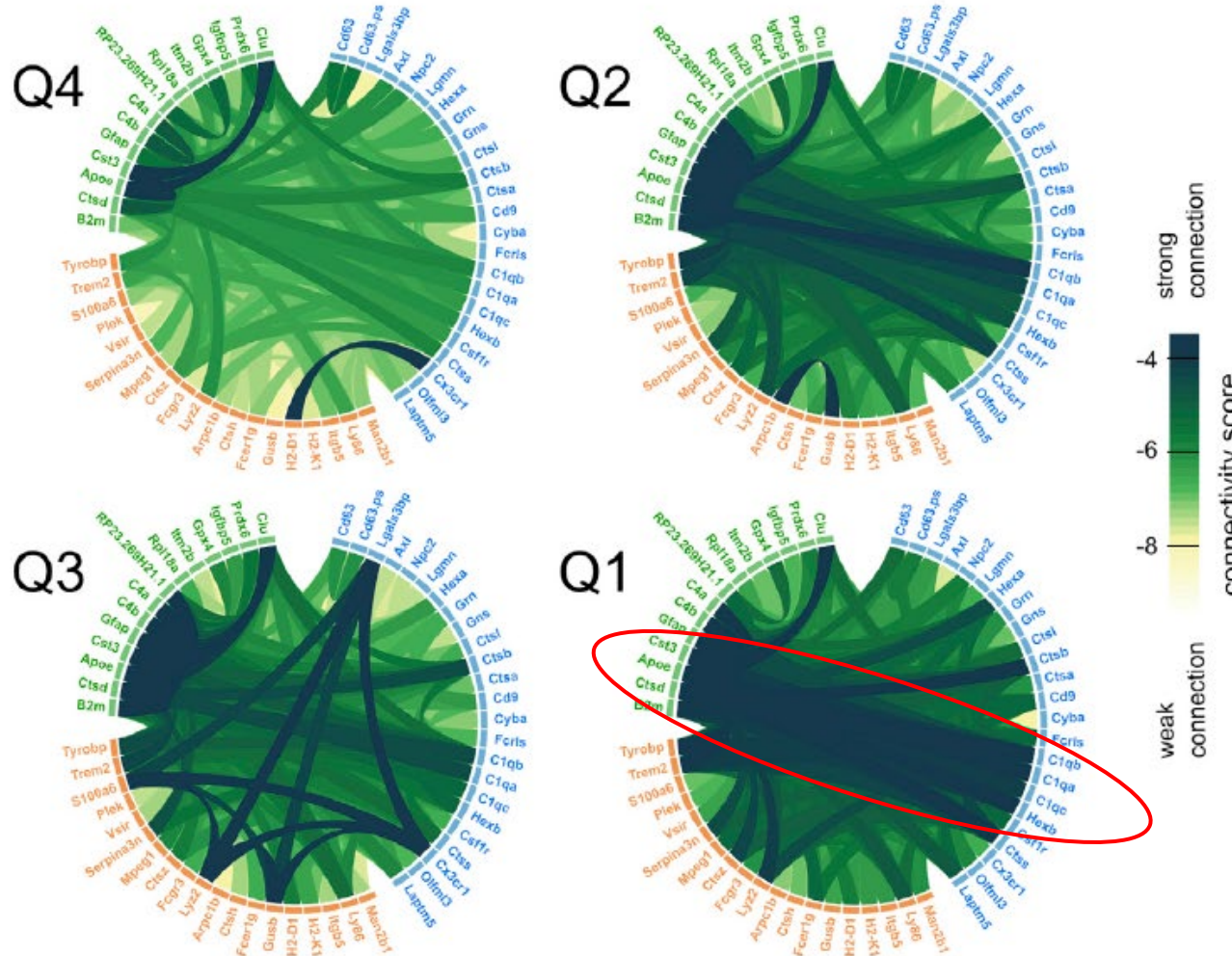
# Cellular signature of PIGs by ISS



- Each punctum is assigned to a cell type by calculating the enrichment in cell-type marker puncta within its 5 um radius
- PIG response to plaque is largely contributed by microglia
- Some PIGs are significantly enriched in several cell types
- Some PIGs switch or start being expressed in different cell types around plaques (*C4a/C4b* and *ApoE*)

# Co-expression of micro and astroglia genes in PIG module

	Q1	Q2	Q3	Q4	
Number of tissue domain	3M	179	338	613	855
	6M	69	57	93	259
	12M	204	150	107	27
	18M	793	699	431	104
	<b>Total</b>	<b>1245</b>	<b>1244</b>	<b>1244</b>	<b>1245</b>
mean of log (A $\beta$ index)	7.70	6.50	5.57	4.73	

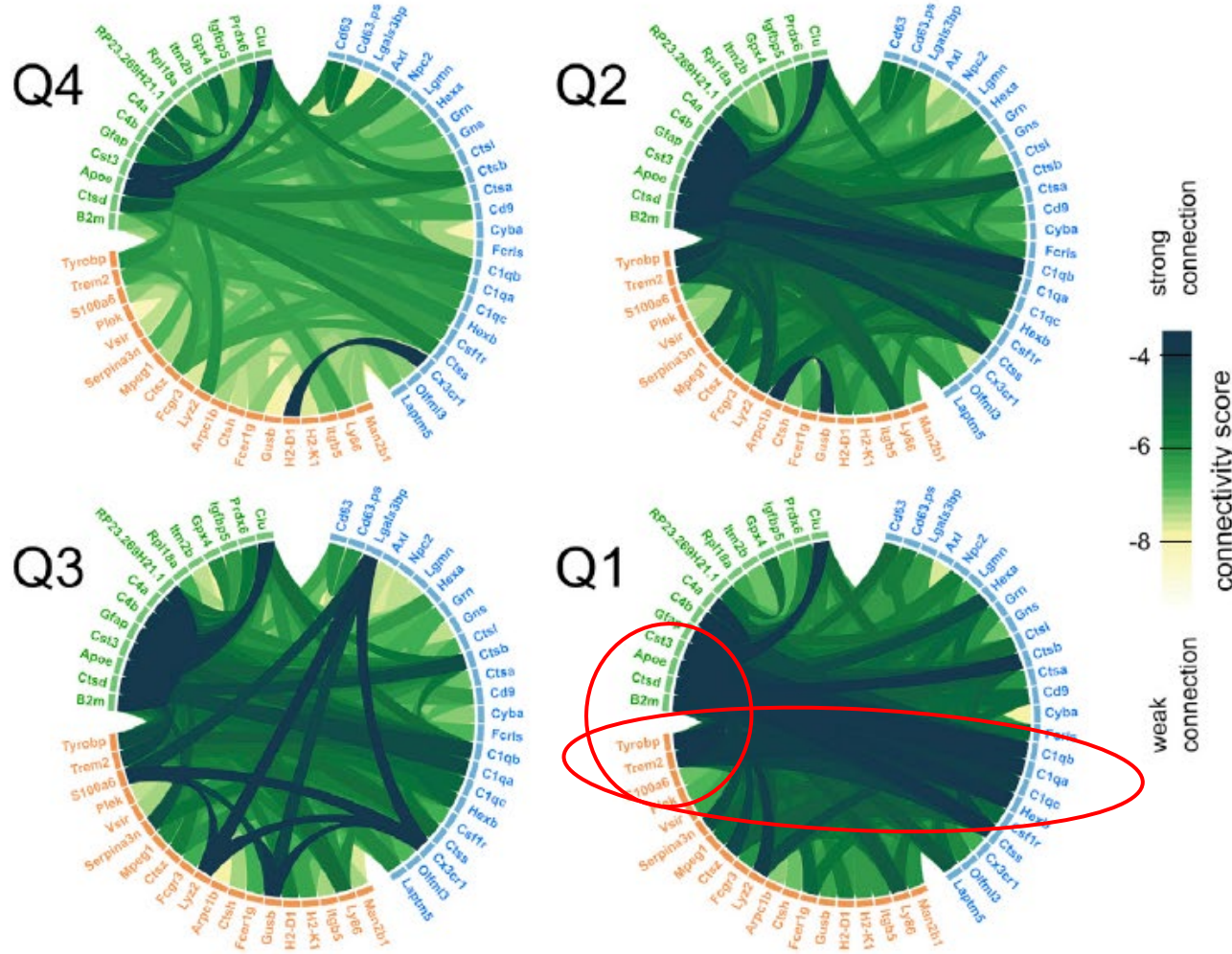


Network analysis on PIGs, separating all ST TDs into WT and four quantiles of AD according to A $\beta$  index

→ The network gradually builds up with increasing A $\beta$  (Q4 lowest amyloid load)

# Co-expression of micro and astroglia genes in PIG module

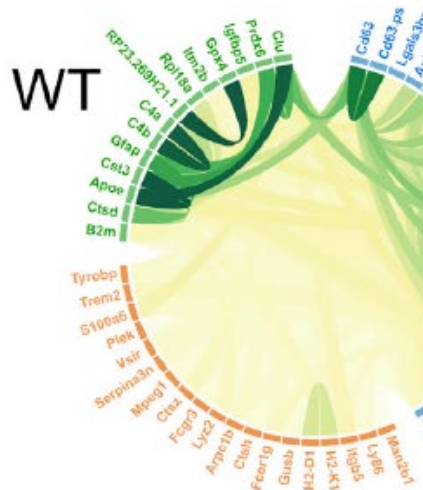
	Q1	Q2	Q3	Q4	
Number of tissue domain	3M	179	338	613	855
	6M	69	57	93	259
	12M	204	150	107	27
	18M	793	699	431	104
	<b>Total</b>	<b>1245</b>	<b>1244</b>	<b>1244</b>	<b>1245</b>
mean of log (A $\beta$ index)	7.70	6.50	5.57	4.73	



Network analysis on PIGs, separating all ST TDs into WT and four quantiles of AD according to A $\beta$  index

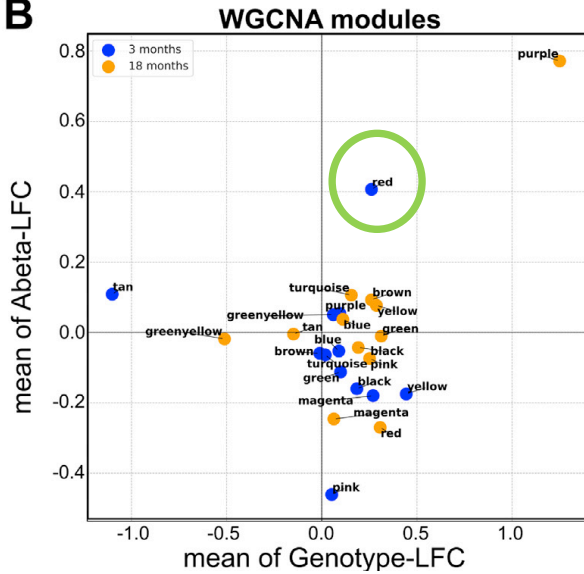
→ The network gradually builds up with increasing A $\beta$  (Q4 lowest amyloid load)

→ The increasing interaction indicates co-expression of genes across different cell types



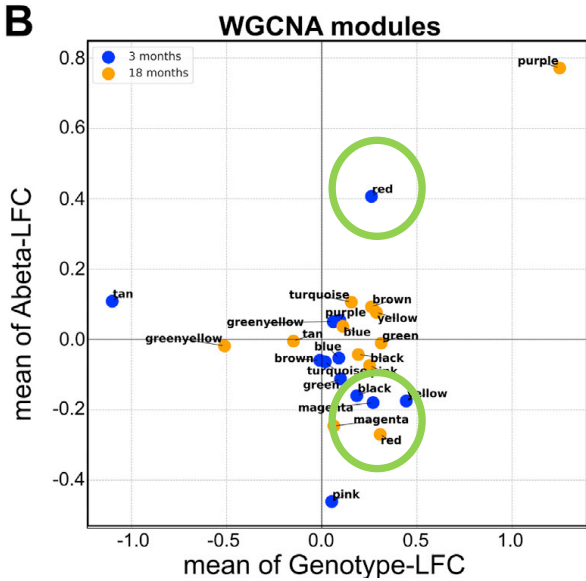
# Oligodendrocytes module (OLIG)

**B**

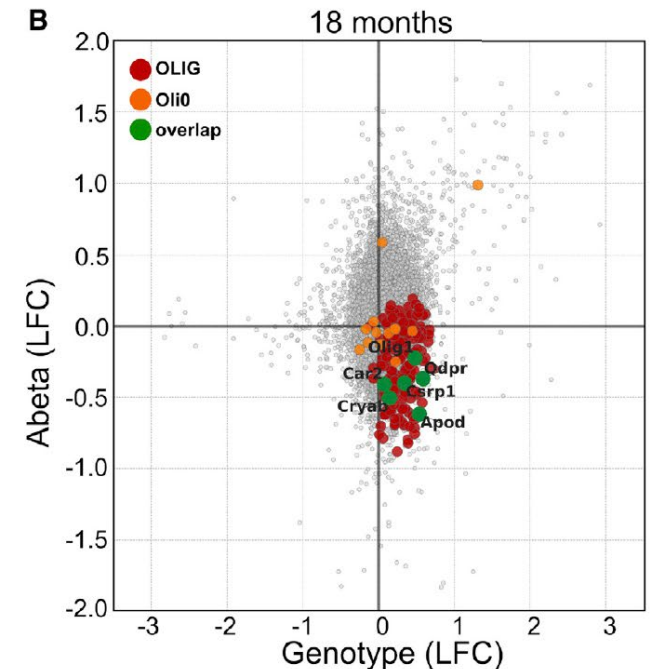
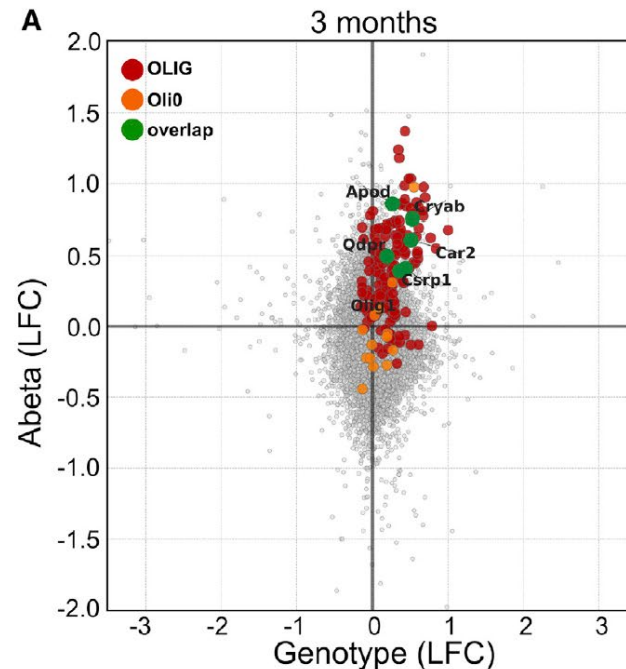


- The top 10 hub genes of the OLIG module are myelin-related transcripts (*Pip1*, *Mbp*, *Mobp*, *Cldn11*, *Mal*, *Apod*, *Cnp*, *Trf*, *Fth1*, and *Plekhb1*)
- Comparing OLIG with published mouse single-cell databases confirms a strong association with oligodendrocytes

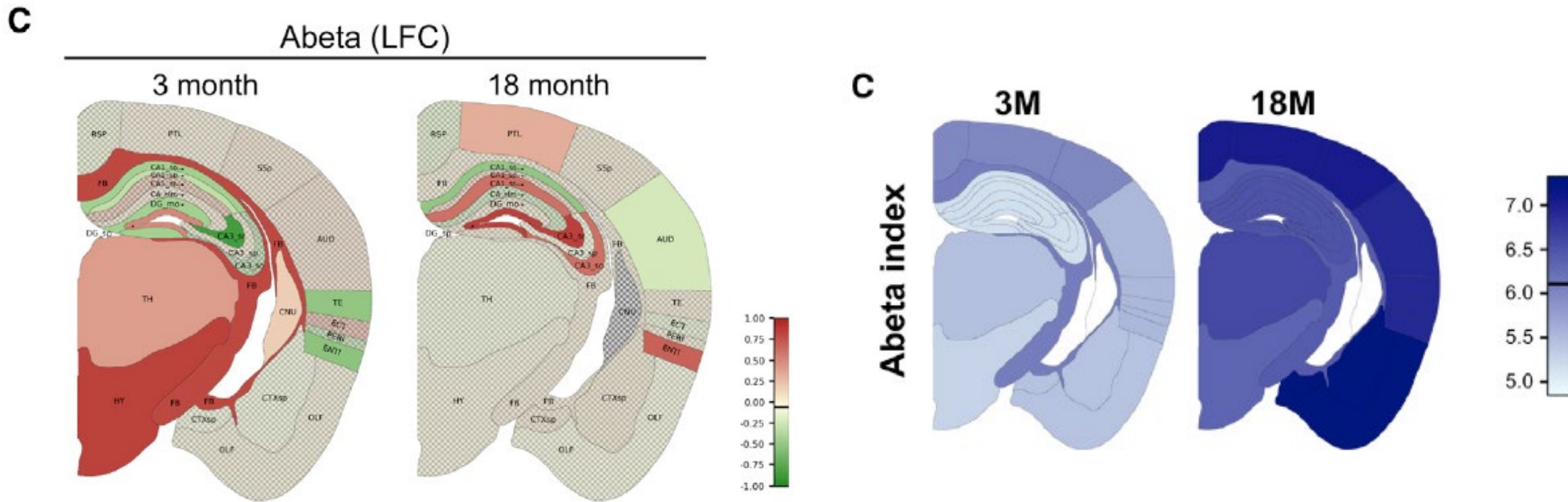
# Oligodendrocytes module (OLIG)



- The top 10 hub genes of the OLIG module are myelin-related transcripts (*Pip1*, *Mbp*, *Mobp*, *Cldn11*, *Mal*, *Apod*, *Cnp*, *Trf*, *Fth1*, and *Plekhb1*)
- Comparing OLIG with published mouse single-cell databases confirms a strong association with oligodendrocytes
- 20 mouse orthologs of human oligodendrocytes markers (*Oli0*). Several *Oli0* orthologs are up- or downregulated together with the OLIG module → correlation with human data



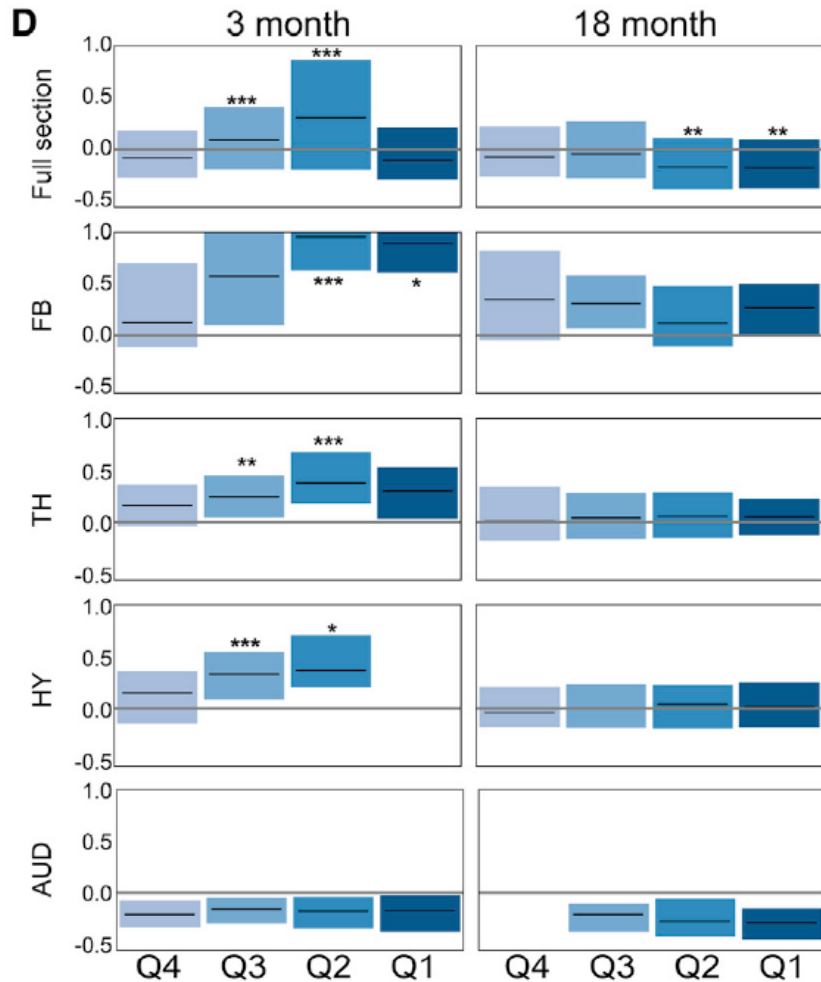
# OLIG module expression variation is not based on amyloid load



When comparing the amyloid profiles in Figure 2C with the OLIG expression profiles there is no overlap:

→ The main driver of OLIG expression is not the  $A\beta$  index but the brain region itself

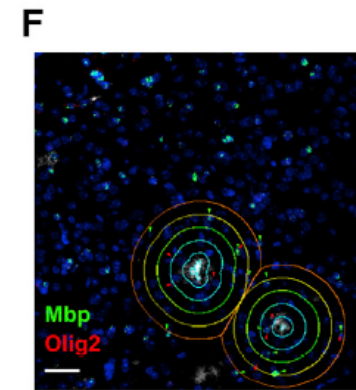
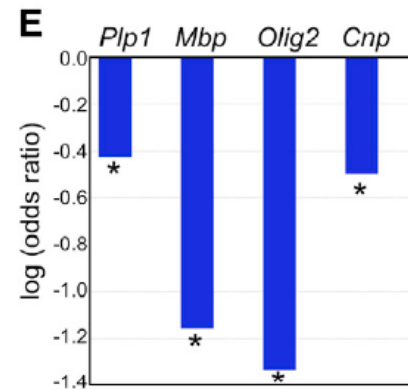
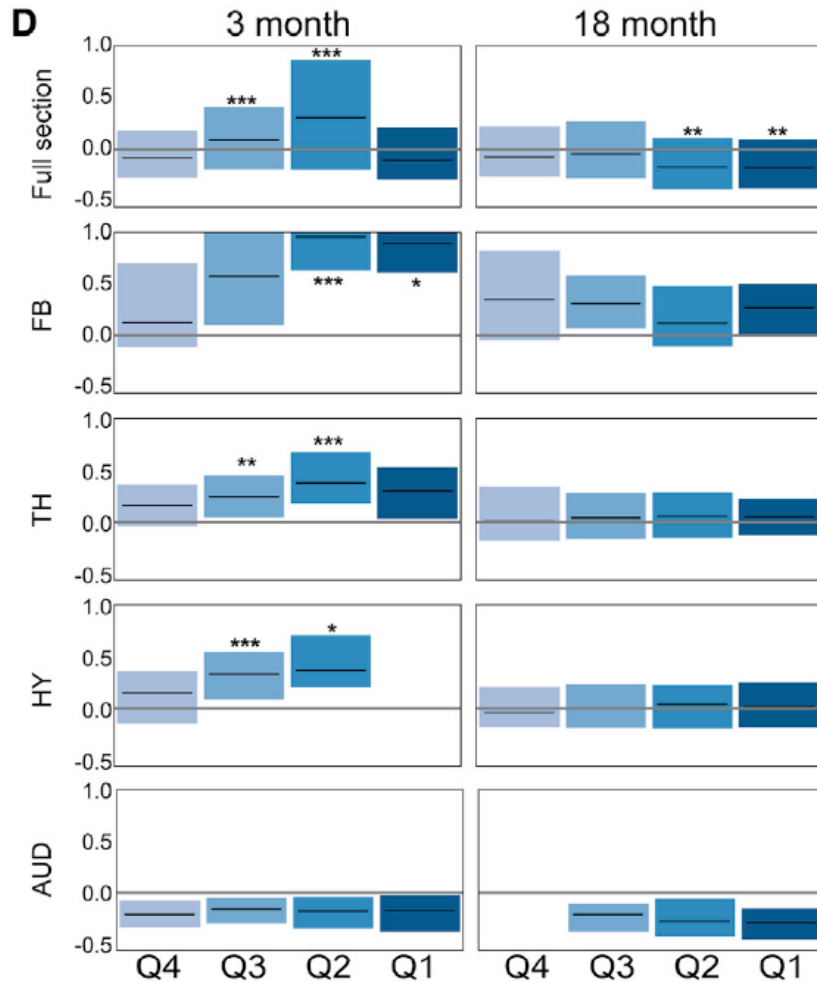
# OLIG module expression variation over time and by brain region



→ OLIG expression at 3 months increases with mild A $\beta$  accumulation in TDs distributed over Q4–Q2

→ Expression of OLIG exhibits a trend toward decreasing in the TDs, with the highest A $\beta$  exposure at 3 months (Q1, which has 21 times more Ab than Q4)

# OLIG module expression variation over time and by brain region

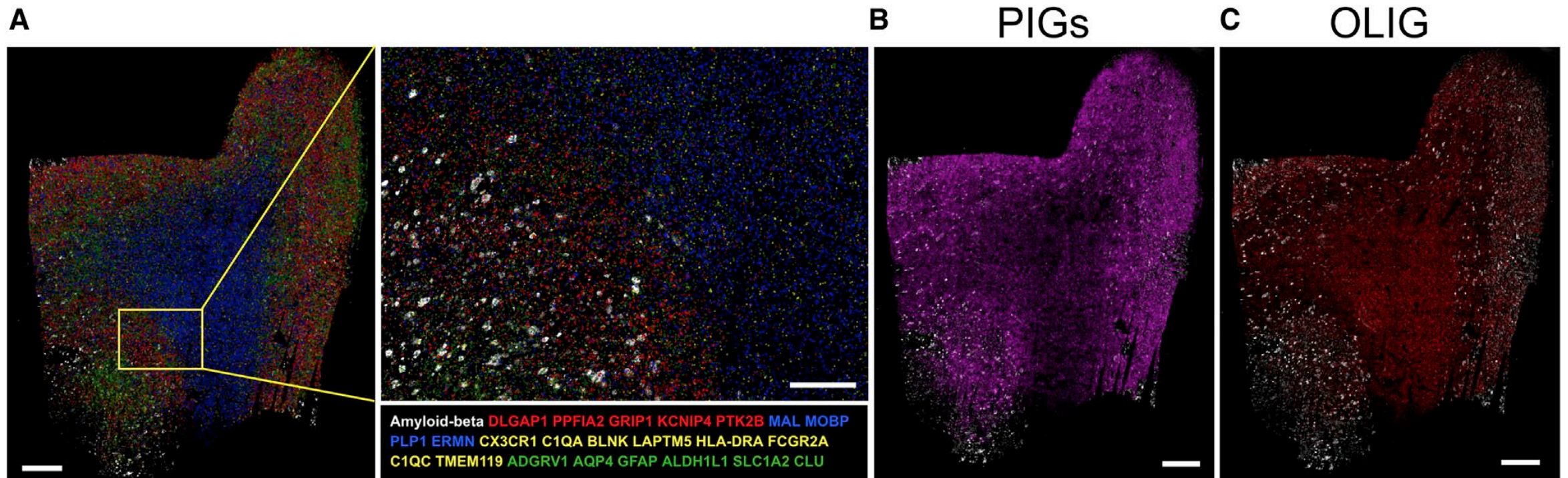


→ OLIG expression at 3 months increases with mild A $\beta$  accumulation in TDs distributed over Q4–Q2

→ Expression of OLIG exhibits a trend toward decreasing in the TDs, with the highest A $\beta$  exposure at 3 months (Q1, which has 21 times more Ab than Q4)

→ RNAscope confirms depletion of 4 OLIGs around dense amyloid plaques already at 3 months

# PIG and OLIG modules in human brains

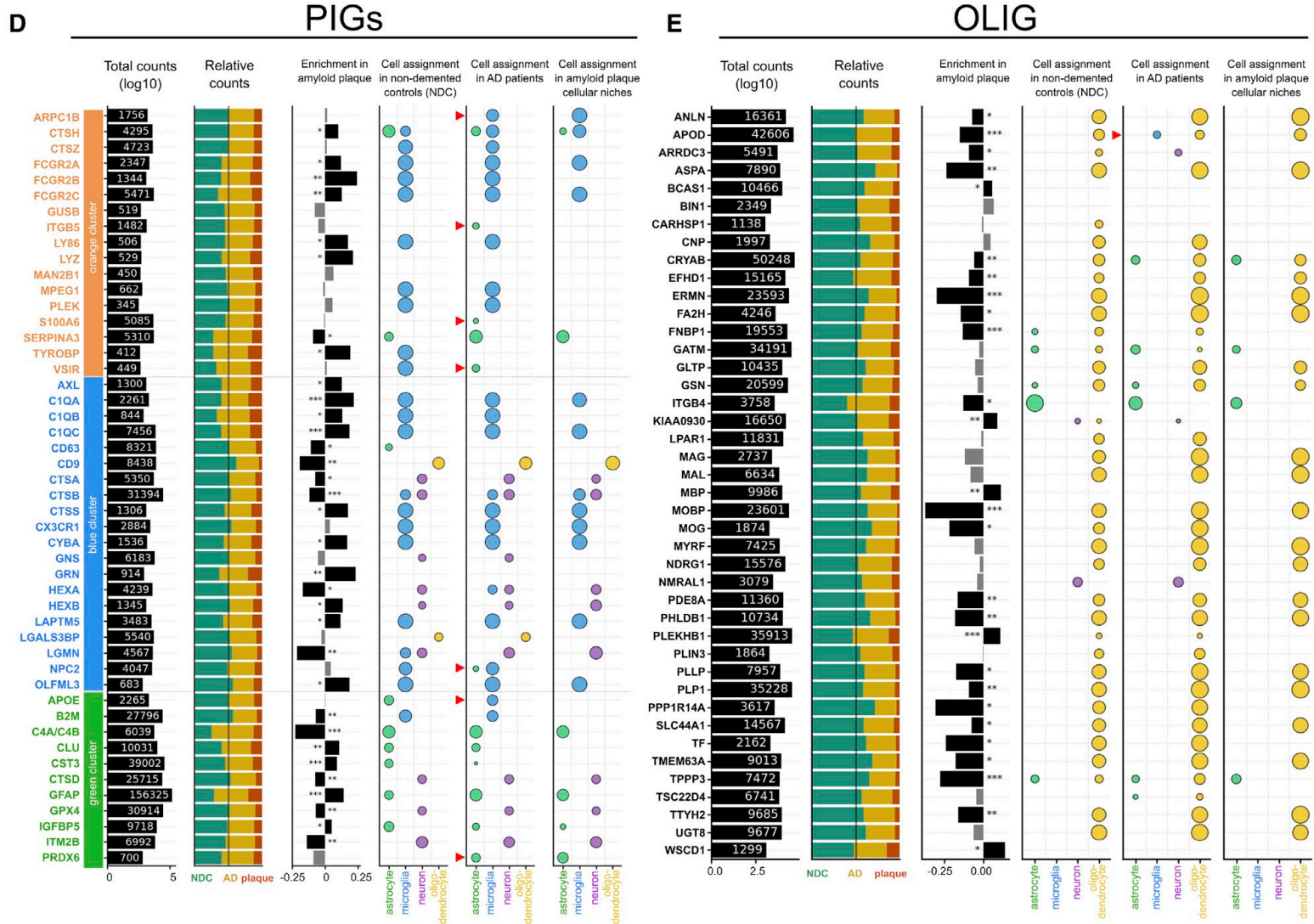


→ Tissue from the superior frontal gyrus

→ 222 gene expression profiles, including 45 human orthologs of PIGs and 42 orthologs of plaque-reactive genes in the OLIG module

→ PIG module and the OLIG are enriched in the grey and white matter respectively

# PIG and OLIG modules in human brains by cell type



→ Within PIGs there was a significant expression of *APOE* and *ARPC1B* in microglia and significant expression of *reactive* astrocytes gene in AD patients but not in controls, indicating disease related glial activation in AD patients

→ Between OLIGs, 22 genes are depleted in the amyloid plaque cellular niches

# AD paper summary

- Combination of ST and ISS investigating AD at a genome-wide scale
  - Identification of PIGs in the microenvironment of plaques representing crosstalk mostly between activated glial cells
  - This network bring alterations to the classical component system (e.g. *C1q*, *C4*) and the endosomal/lysosomal pathways (e.g. *Grn*, *Gns*, *Ctsa*)
  - Identification of OLIG module, enriched in genes involved in myelination, is downregulated with higher amyloid load
  - Correlation of gene alteration between mouse models and AD patients
- **Amyloid plaques induce a coordinated response of all cell types in the A $\beta$  plaque cellular niche**
- **Can removal of plaques reverse these ongoing cellular processes?**

# Overall ST conclusions

- ST is a powerful tool to understand transcriptome wide changes in both entire tissue slices or around specific regions of interest (e.g. plaques)
- ST data analysis can give morphological and pathological information about the tissue → important when looking at networks in specific cells types perturbed by the disease
- It can be associated to IHC and ISS for single cell resolution (although newer techniques have reached single cell resolution!)
- Can be performed on paraffin fixed tissues (no problem with biosafety)

**Thank you for your attention!**  
**Questions?**

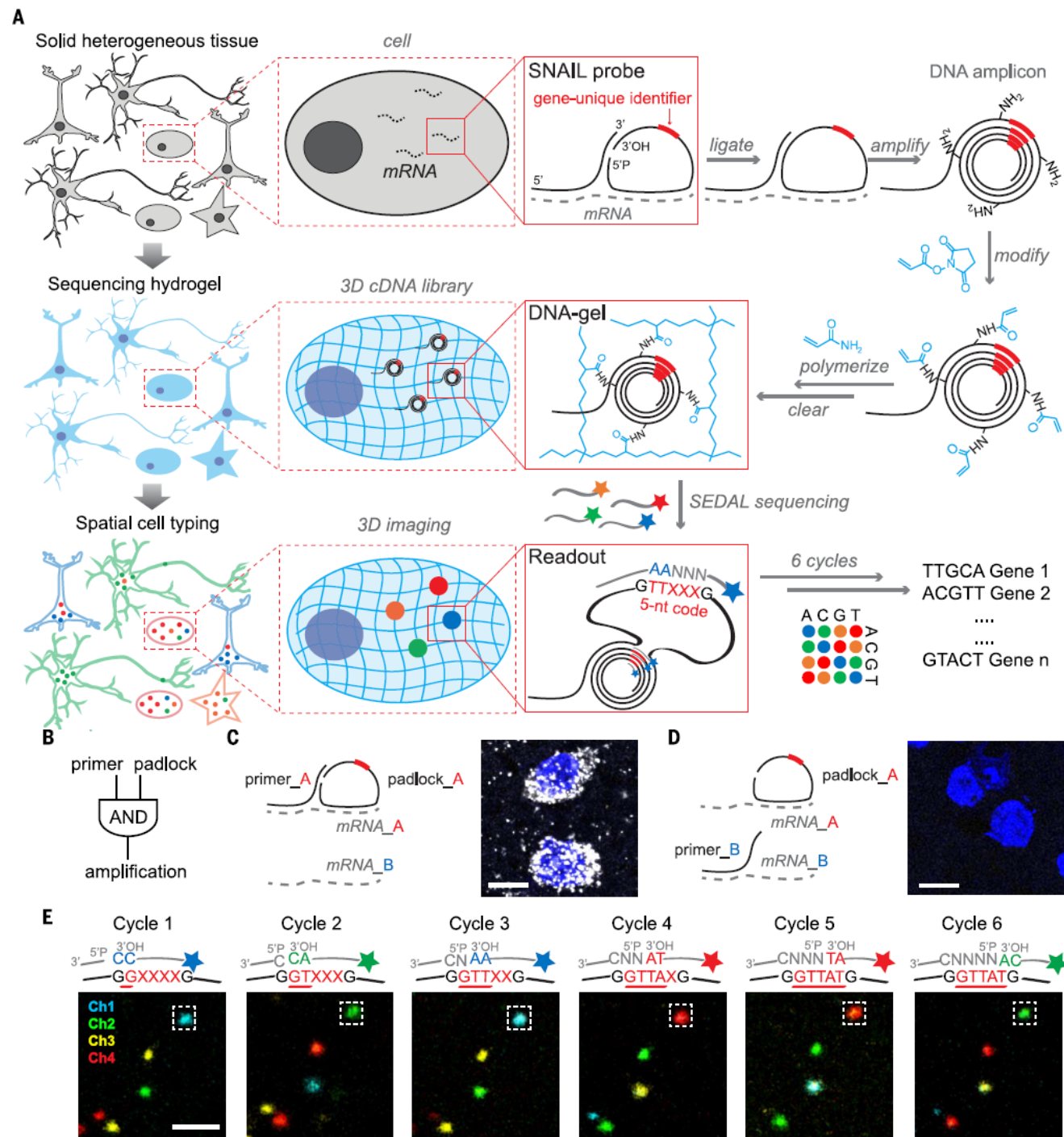


# STARmap

A) STARmap overview schematic. After brain tissue is prepared the custom SNAIL probes that encounter and hybridize to intracellular mRNAs within the intact tissue are enzymatically replicated as cDNA amplicons. The amplicons are constructed in situ with an acrylic acid N-hydroxysuccinimide moiety modification (blue) and then copolymerized with acrylamide to embed within a hydrogel network. Each SNAIL probe contains a gene-specific identifier segment (red) that is read-out through in situ sequencing with two-base encoding for error correction (SEDAL). Last, highly multiplexed RNA quantification in three dimensions reveals gene expression and cell types in space.

B) SNAIL logic. A pair of primer and padlock probes amplifies target specific signals and excludes noise known to commonly arise from nonspecific hybridization of a single probe.

C) and D) Only adjacent binding of primer and padlock probes leads to signal amplification.



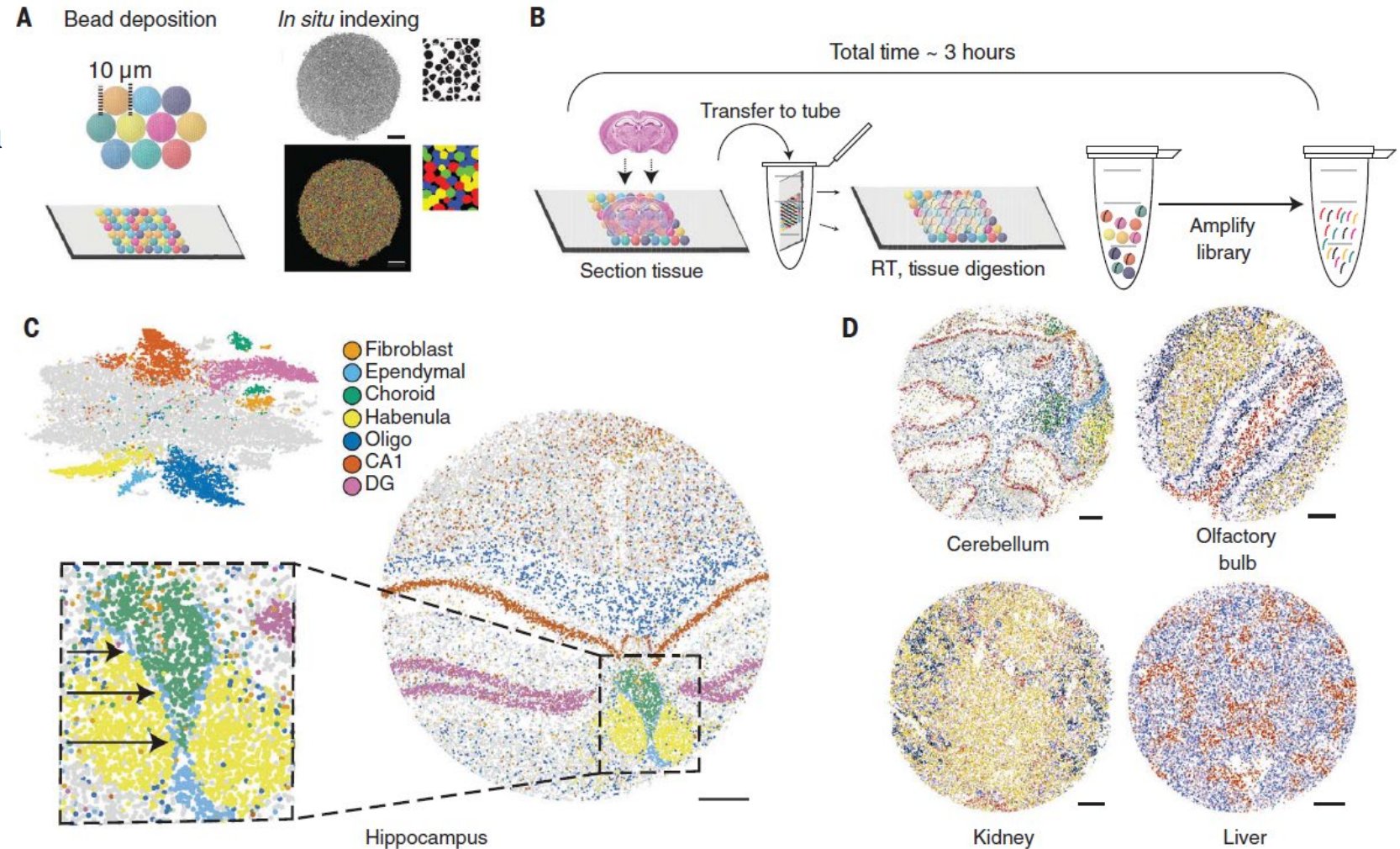
# Other examples of ST protocols: Slide-Seq

## Slide-seq: A scalable technology for measuring genome-wide expression at high spatial resolution

Samuel G. Rodriques<sup>1,2,3\*</sup>, Robert R. Stickels<sup>3,4,5\*</sup>, Aleksandrina Goeva<sup>3</sup>, Carly A. Martin<sup>3</sup>, Evan Murray<sup>3</sup>, Charles R. Vanderburg<sup>3</sup>, Joshua Welch<sup>3</sup>, Linlin M. Chen<sup>3</sup>, Fei Chen<sup>3,†,‡</sup>, Evan Z. Macosko<sup>3,6,†,‡</sup>

*Science* **363**, 1463–1467 (2019)

- Unbiased transcriptome-scale profiling on large areas
- Use on densely barcoded bead arrays indexed before placing the tissue on them
- Near to cellular resolution (10 $\mu$ m vs 55 with 10x genomics)

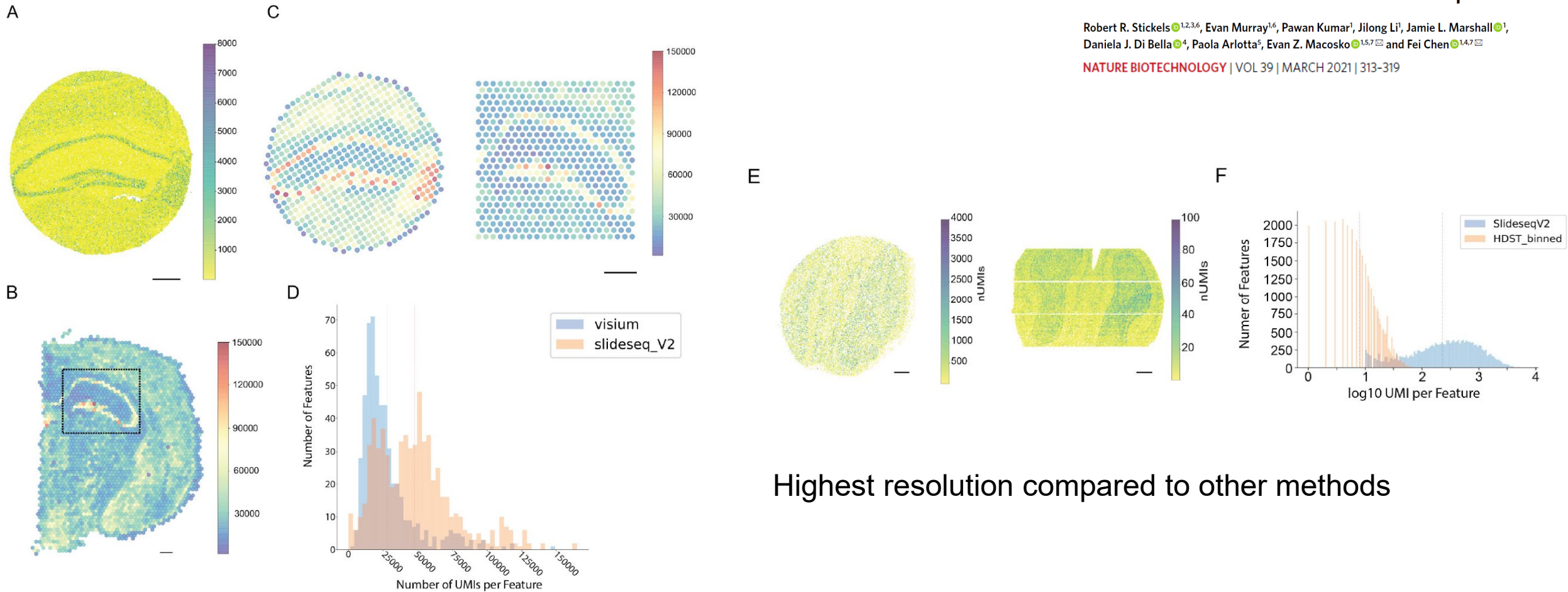


# Slide-SeqV2 vs 10x Visium and HDST

Highly sensitive spatial transcriptomics at near-cellular resolution with Slide-seqV2

Robert R. Stickels<sup>1,2,3,6</sup>, Evan Murray<sup>1,6</sup>, Pawan Kumar<sup>1</sup>, Jilong Li<sup>1</sup>, Jamie L. Marshall<sup>1</sup>, Daniela J. Di Bella<sup>4</sup>, Paola Arlotta<sup>5</sup>, Evan Z. Macosko<sup>1,5,7</sup> and Fei Chen<sup>1,4,7</sup>

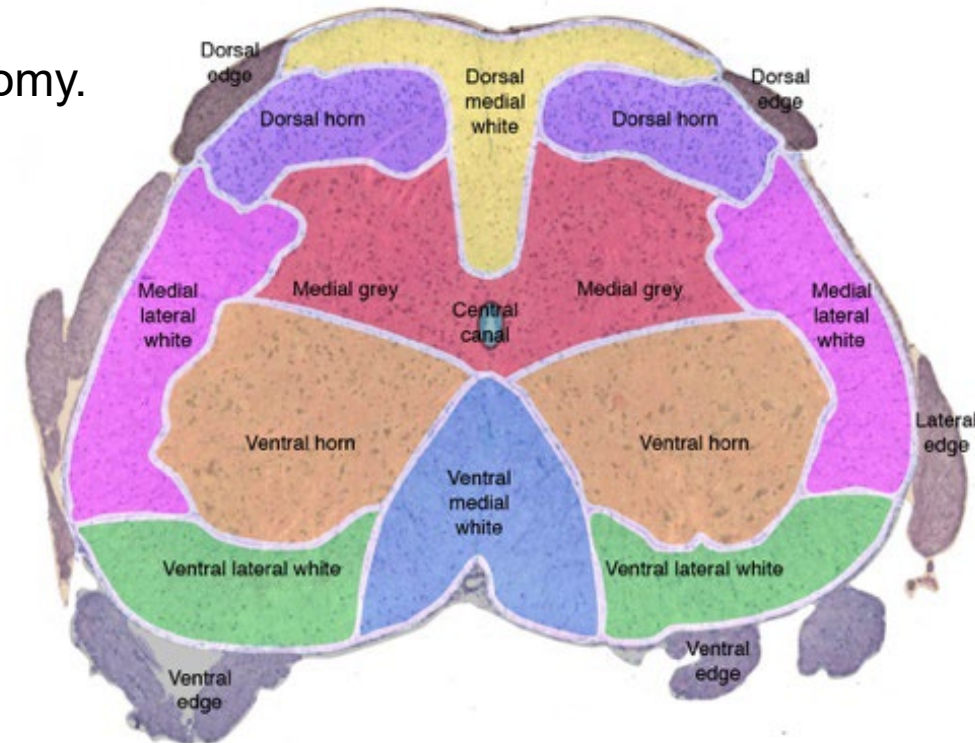
NATURE BIOTECHNOLOGY | VOL 39 | MARCH 2021 | 313-319



Highest resolution compared to other methods

# Amyotrophic lateral sclerosis

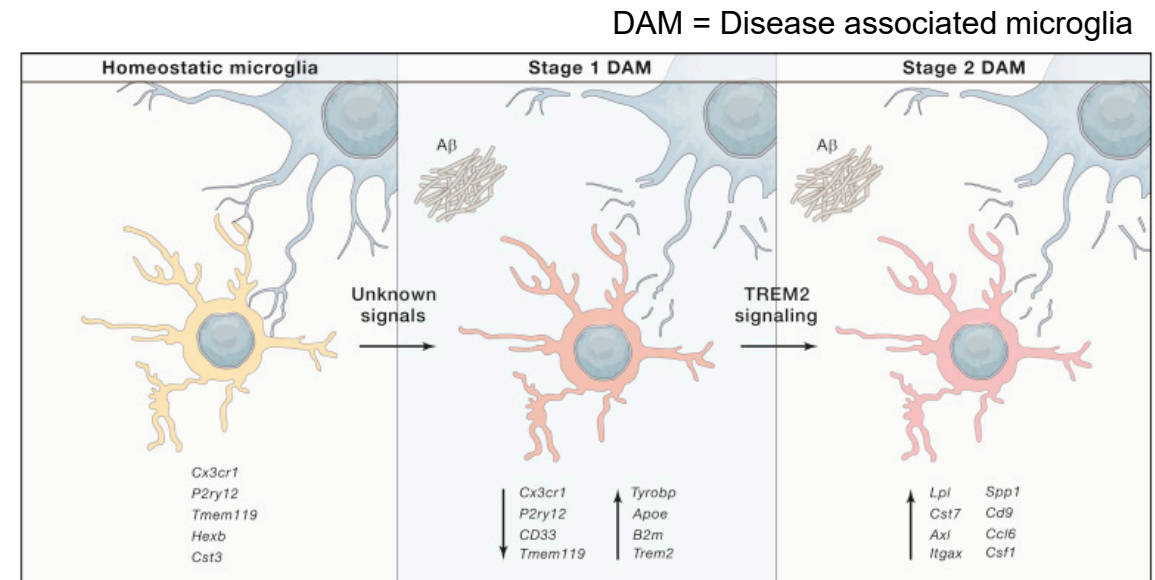
- ALS is a neurodegenerative disease of motor neurons, beginning from the distal ones (innervating limbs) and progressively causing total paralysis
- We still do not know the mechanisms initiating the disease
- It is possible that motor neurons-glia cells interaction might be at the base of this
- Spinal cord is easy to analyze thanks to its spatially organized anatomy.



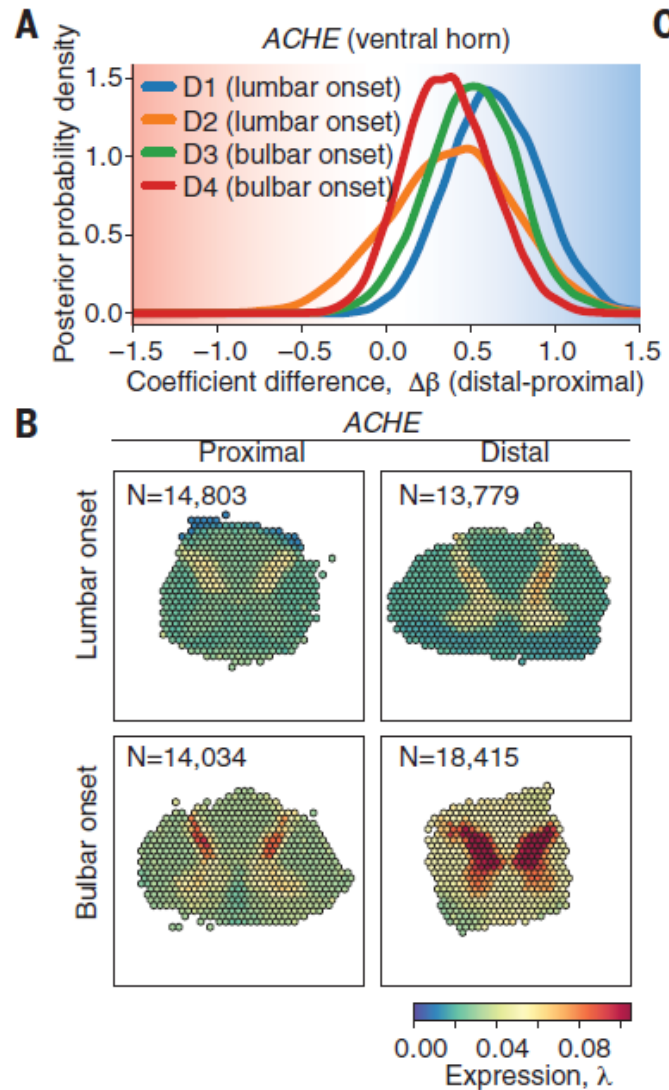
# Understanding spatiotemporal dynamics of microglia activation

Use of TREM2, often reported in other neurodegenerative diseases (AD, ALS, MS):

- TREM2 and TYROBP form a receptor complex that can trigger phagocytosis or modulate cytokine signalling
- This mechanism also involves *ApoE*, *Lpl*, *B2m*, and *Cx3cr1* and is activated by microglial phagocytosis of apoptotic neurons



# *ACHE* activity is linked to neuromuscular defects in ALS

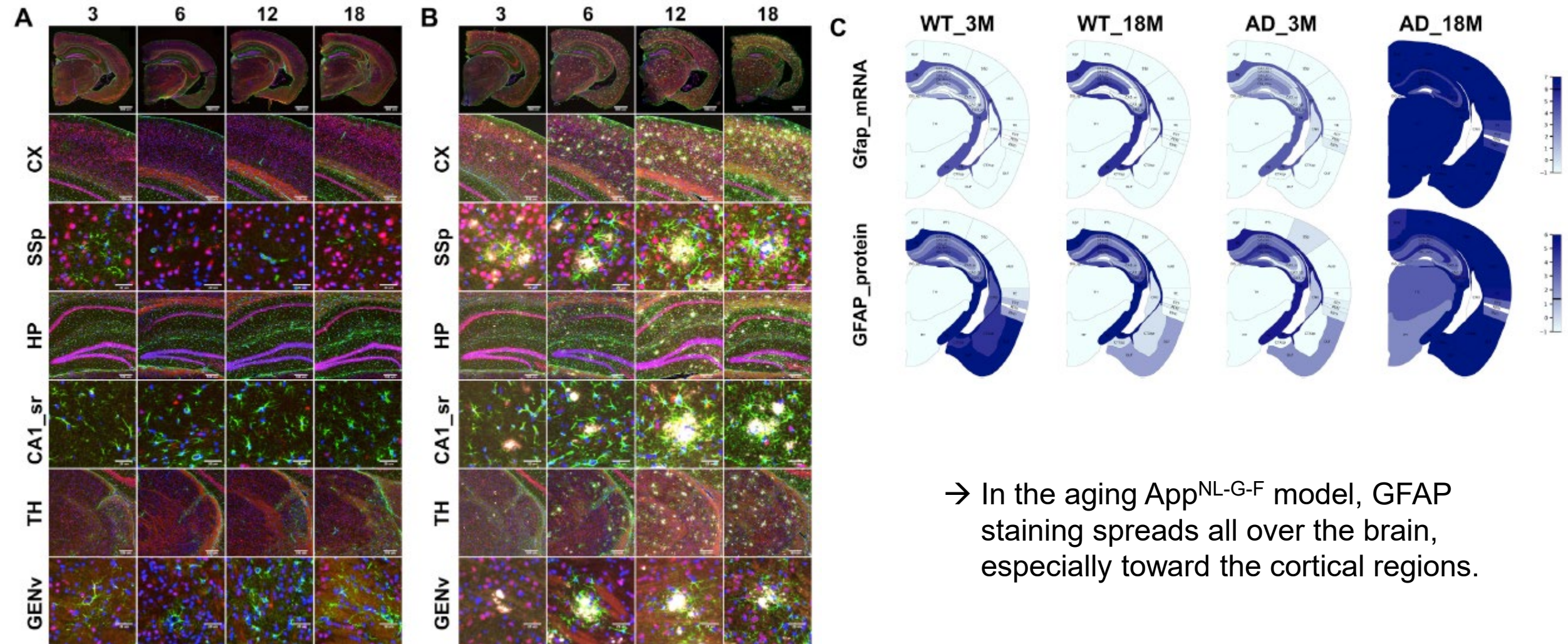


The severity of ALS pathology is related to proximity to site of symptom onset

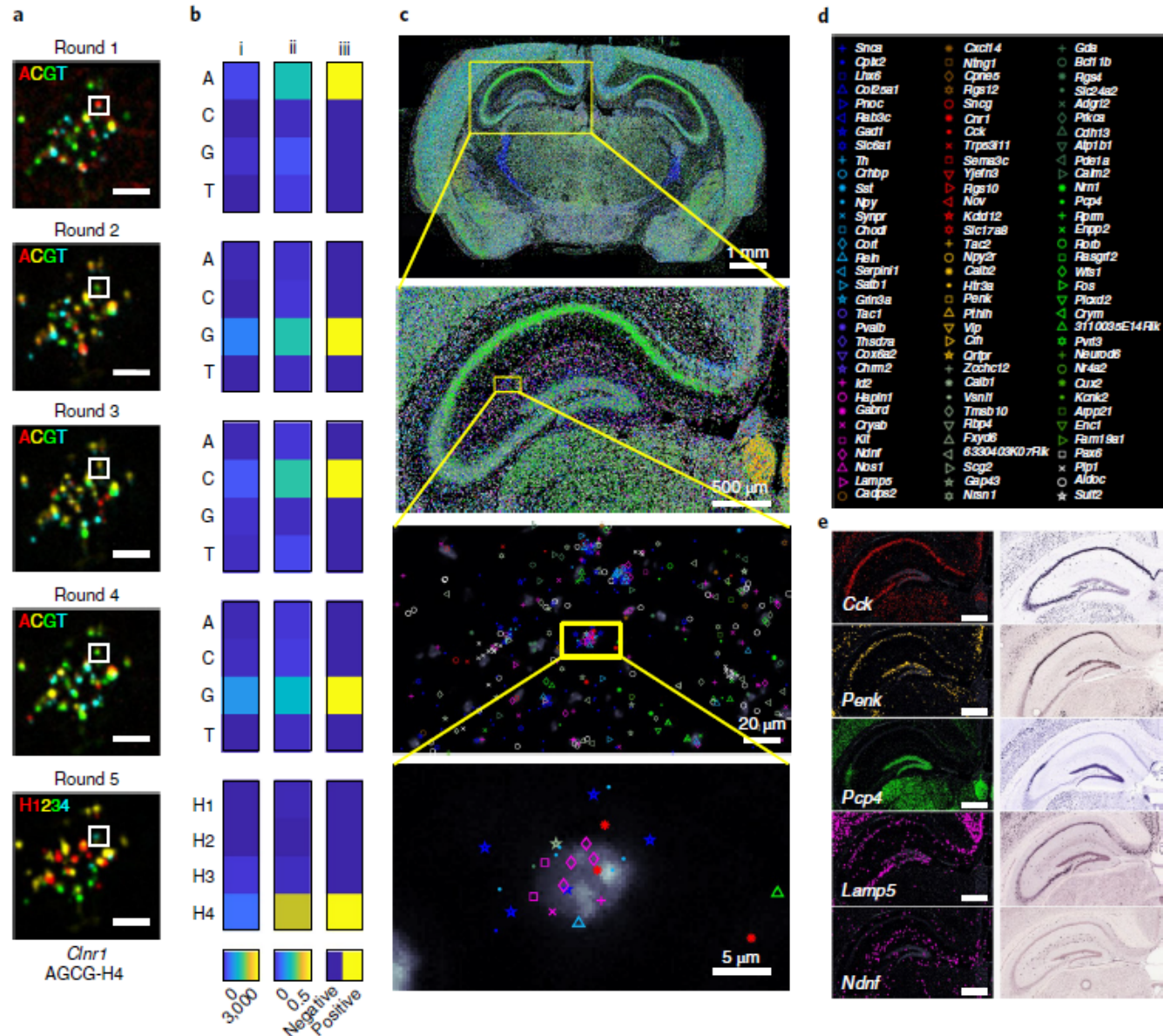
→ Analysis of ventral horns coefficients for *ACHE* per patient (D1 to D4). Calculation of differences between distal and proximal region with respect to the onset location.

→ Achetylcholinesterase (*ACHE*) shows reduced expression at locations proximal to spinal segments innervating the site of symptom onset

# Higher A $\beta$ load = higher astrogliosis



# ISS extra info



Padlock probes were designed for the selected genes, each containing two arms together matching a 40-base-pair (bp) sequence on the cDNA, a 4-bp barcode, an 'anchor sequence' allowing all amplicons to be labeled simultaneously and a 20-bp hybridization sequence for additional readouts.